Chapter 8

Scheduling of EV battery swapping in microgrids ☆

Pengcheng You
Whiting School of Engineering, Johns Hopkins University, Baltimore, MD, United States

1 Introduction

1.1 Background, motivation, and contributions

We are at the cusp of a historic transformation of our energy system into a more sustainable form in the coming decades. Electrification of our transportation system will be an important component because vehicles today consume more than a quarter of energy in the United States and emit more than a quarter of energy-related carbon dioxide [3]. Electrification will not only greatly reduce greenhouse gas emission, but also have a large impact on the future grid because electric vehicles (EVs) are large but flexible loads [4]. The impact of EVs is especially significant for microgrids that group locally interconnected loads and distributed energy resources and act as an individual controllable entity either to interact with the main grid in the grid-connected mode or stand alone in the island mode. A microgrid is therefore an effective paradigm to integrate various sources of renewables by fully utilizing its dispatchable elements, among which EVs could play a momentous role. EVs, as *moving storage* in essence, readily realize energy/power shift in both temporal and spatial domains by their routine running and charging. It is foreseeable that a huge amount of flexibility can be exploited from EV operation to complement microgrid operation.

As we will see in this chapter, there is a large literature on various aspects of EV charging. It is widely believed that uncontrolled EV charging may stress or even disrupt power grids, but well-controlled charging can help stabilize grids and integrate renewables. However, we look at EV operation from a different angle here (i.e., battery swapping). Instead of charging its battery when an EV is running out of energy, it could have the depleted battery swapped at a service station by a fully charged battery so as to avoid suffering the

☆ This chapter basically summarizes and extends the work in [1, 2] to the context of a microgrid.

Distributed Control Methods and Cyber Security Issues in Microgrids
https://doi.org/10.1016/B978-0-12-816946-9.00008-6

problem of long waits. All unloaded batteries are charged centrally at service stations to prepare for future battery swapping demand. Battery swapping as a refueling model for EVs, dating back to 2007 when it was first commercialized by a start-up *Better Place* in Israel, has been reemerging in recent years with major advances in battery charging and energy storage. Other than technological innovation, operational breakthrough is another critical factor that contributes to the bloom of battery swapping. Technically, this mechanism is implementable with pilot programs already established in Israel and China. Its advantages are fourfold. First, it takes only minutes to swap a battery but often hours to recharge it. Second, the aggregation of charging loads reduces demand uncertainty compared with individual EV charging, simplifying power system operation. Third, the aggregation of charging loads endows service stations with greater flexibility in scheduling battery charging and providing ancillary services. Fourth, batteries, as the most costly core of an EV, can be leased rather than purchased, tremendously lowering the expenditure for EV owners.

In the meantime, battery swapping is also faced with unique challenges in popularization. First, it requires standardization of vehicles, batteries, and swapping infrastructure, which has proven to be difficult. Second, a business model is needed to address ownership, maintenance, and payment issues regarding shared batteries. However, the problem we will study in this chapter circumvents these obstacles and mainly focuses on an EV-station battery swapping system supplied by a microgrid and its interactions, motivated by a novel battery swapping model currently being pursued in China, especially for electric buses and taxis [5]. The State Grid (one of the two national utility companies) of China is experimenting with this model where it operates not only the power grid, but also service stations and a taxi service around a city, which constitute a vertically integrated system. When the state of charge of a State Grid taxi is low, it goes to one of the State Grid operated service stations to exchange its depleted battery for a fully charged one. While battery swapping takes only a few minutes, it is not uncommon for taxis to arrive at a service station, only to find that it runs out of fully charged batteries and there is a queue of taxis waiting to swap their batteries. The occasional multihour waits are a serious impediment that degrades the efficiency of battery swapping, which is predicated on having sufficient fully charged batteries at service stations. In fact, it is often the case that some service stations which EVs gather around run short of fully charged batteries quickly while others accrue more and more. Obviously it is neither economical nor practical to stock enough batteries at every service station to serve the worst-case EV arrival patterns. This indicates that EVs have the incentive to choose service stations so as to avoid long waits. On the other hand, microgrid operation is also tremendously influenced by EVs' battery swapping decisions since battery charging loads are redistributed spatially in the network, which is rich in load flexibility and bound to improve the system operating efficiency if well managed.

To this end, in this chapter we propose to coordinate battery swapping in a microgrid such that EVs can make the most efficient use of currently available batteries in the system and meanwhile the microgrid operation is jointly optimized. Specifically, we formulate in Section 2 an optimal scheduling problem for battery swapping in a microgrid that assigns to each EV a best station to swap its depleted battery based on its current location and state of charge. The station assignments not only determine EVs' travel distance, but also impact significantly the power flows on the microgrid because batteries are large loads. The schedule aims to minimize a weighted sum of EVs' travel distance and electricity generation cost over both station assignments and power flow variables, subject to EV range constraints, grid operational constraints, and AC power flow equations.

This joint battery swapping and optimal power flow (OPF) problem is nonconvex and computationally difficult for two reasons. First, AC power flow equations are nonlinear. Second, the station assignment variables are binary. We address the first difficulty in Section 2.1 by summarizing several representative linearization/convexification methods to approximate/relax the nonlinear power flow equations that prove to be accurate and effective given different network topologies or parameterization. Fixing any station assignments, the remaining OPF problem is then convex. The second difficulty can be properly addressed in two fashions. The centralized solution in Section 3 applies generalized Benders decomposition to the current mixed-integer convex program, and is suitable for cases where the microgrid, service stations, and EVs are managed centrally by the same operator (e.g., the State Grid model). Supposing an exact underlying linearization/relaxation of the power flow equations is given, the generalized Benders decomposition computes a global optimum in reasonable time. In this centralized solution, the operator needs global information such as the grid topology, impedances, operational constraints, background loads, availability of fully charged batteries at each station, locations and states of charge of EVs, etc. It is implementable only in a vertically integrated system like the State Grid operated electric taxi program.

As EVs proliferate and battery swapping matures, an equally (if not more) likely model will emerge where the microgrid is managed by a utility company, service stations are managed by a station operator (or multiple station operators), and EVs may be managed by individual drivers (or multiple EV groups, e.g., taxi companies in the electric taxi case). In particular, the set of EVs to be scheduled may include a large number of private cars in addition to commercial fleet vehicles. They may not be willing to share their private information. The centralized solution will fail to apply for these future scenarios. Moreover, generalized Benders decomposition solves a mixed-integer convex program centrally and is still computationally expensive. It is hard to scale to compute in real-time optimal station assignments and an (linearized/relaxed) OPF solution when the numbers of EVs and stations are large.

To this end, we develop scalable distributed solutions that preserve private information and are more suitable for general scenarios. Instead of generalized Benders decomposition, we relax the binary station assignment variables to real variables in [0, 1]. With both the linearization/relaxation of power flow equations and the relaxation of binary variables, the resulting approximate problem of joint battery swapping and OPF is a convex program. This allows us to develop two distributed solutions where separate entities make their individual decisions but coordinate through information exchanges that do not involve their private information in order to solve jointly the global problem.

The first solution, based on the alternating direction method of multipliers (ADMM), is for systems where the microgrid is managed by a utility company and all service stations and EVs are managed by a station operator. Here the utility company maintains a local estimate of some *aggregate* assignment information that is computed by the station operator, and they exchange the estimate and the aggregate information to attain consensus. The second solution, based on dual decomposition, is for systems where the microgrid is managed by a utility company, all service stations are managed by a station operator, and all EVs are individually operated. The utility company still sends its local estimate to the station operator while the station operator does not need to send the utility company the aggregate assignment information, but only some Lagrange multipliers. The station operator also *broadcasts* Lagrange multipliers to all EVs and individual EVs respond by sending the station operator their choices of stations for battery swapping based on the received Lagrange multipliers and their current locations and driving ranges. In both approaches, given the aggregate assignment information and Lagrange multipliers that are exchanged, different entities only need their own local states (e.g., power flow variables) and local data (e.g., impedance values, battery states, EV locations, and driving ranges) to compute iteratively their own decisions. See Fig. 1 for the distributed framework.

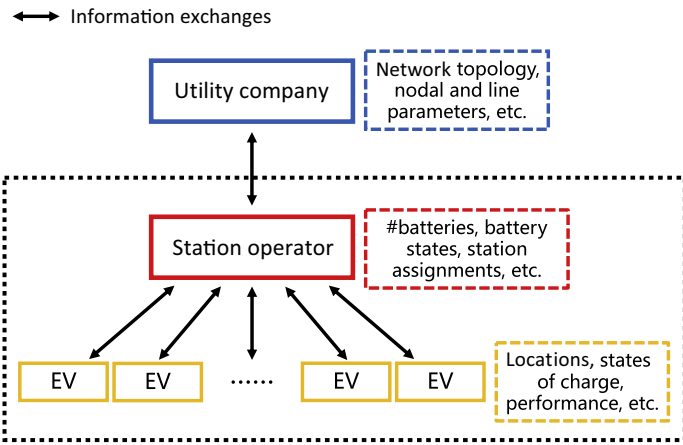

Fig. 1 Distributed framework.

Suppose an exact underlying linearization/relaxation of the power flow equations is given; the proposed distributed algorithms, however, may return station assignments that are not binary due to the relaxation of binary variables, which suggest a probabilistic station assignment for an EV. We prove an upper bound on the number of such EVs with nonbinary station assignments. The bound guarantees that the discretization can be readily implemented and also justifies the final solution is close to optimum.

In Section 5, we illustrate the performance of our centralized and distributed solutions through simulations on a real 56-bus test system from Southern California Edison (SCE). The simulation results suggest that the centralized solution is effective and computationally tractable for practical application, and the distributed solutions are scalable and usually achieve satisfactory station assignments under real conditions.

1.2 Literature

There is a large literature on EV charging, for example, optimizing charging schedule for various purposes such as demand response, load profile flattening, or frequency regulation [6–9]; architecture for mass charging [10–13]; locational marginal pricing for EV charging [14, 15]; and the interaction between EV penetration and the optimal deployment of charging stations [16].

Sojoudi et al. [17] seem to be the first to optimize jointly EV charging and AC power flow spatially and temporally through semidefinite relaxation. Zhang et al. [18] extend the joint OPF-charging problem to multiphase distribution networks and propose a distributed charging algorithm based on ADMM. Chen et al. [19] decompose the joint OPF-charging problem into an OPF subproblem that is solved centrally by a utility company and a charging subproblem that is solved in a distributed manner by individual EVs through a coordinative valley-filling signal from the utility company. De Hoog et al. [20] use a linear model and formulate EV charging on a three-phase unbalanced grid as a receding horizon optimization problem. It shows that optimizing the charging schedule can increase the EV penetration that is sustainable by the grid from 10%–15% to 80%. Linearization is also used in [21] to model EV charging on a three-phase unbalanced grid as a mixed-integer linear program. The binarity arises from the fact that an EV is either being charged at its peak rate or off. These papers focus on jointly optimizing power flows and charging for EVs connected to given locations on the grid. A key feature of battery swapping scheduling is, however, the use of EV mobility to optimize explicitly the spatial redistribution of charging loads.

The literature on battery swapping is much smaller. Tan et al. [22] propose a mixed queuing network that consists of a closed queue of batteries and an open queue of EVs to model the battery swapping processes, and analyze its steady-state distribution. Yang et al. [23] design a dynamic operation model of a battery swapping station and put forth a bidding strategy in power markets.

You et al. [24] study the optimal charging schedule of a battery swapping station serving electric buses and propose an efficient distributed solution that scales with the number of charging boxes in the station. Sarker et al. [25] propose a day-ahead model for the operation of battery swapping stations and use robust optimization to deal with future uncertainty of battery demand and electricity prices. Zheng et al. in [26] study the optimal design and planning of a battery swapping station in a distribution system to maximize its net present value, taking into account life cycle cost of batteries, grid upgrades, reliability, operational cost, and investment cost. Zhang et al. [27] discuss several business models of battery swapping and leasing service in China. You et al. [28–30] present a series of work on station assignment for EV battery swapping to make better use of batteries in practical application. However, the impact of the assignments on power systems is not taken into account. To the best of our knowledge, joint optimization of battery swapping and power flows on microgrids has not been investigated, which is becoming an emerging practical issue.

The distributed solutions are motivated by the need to preserve private information of different entities operating microgrids, stations, and EVs. Privacy in future grids is a key challenge facing both utilities and end users [31], for example, see [32–35] for privacy concerns on smart meters and [36–38] for privacy concerns on EVs. Distributed algorithms preserve privacy as global information is not needed for local computations. Liu et al. [34] schedule thermostatically controlled loads and batteries in a household to hide its actual load profiles such that no sensitive information can be inferred from electricity usage. Yang et al. [35] design an online control algorithm of batteries that only uses the current load requirement and electricity price to optimize the tradeoff between smart meter data privacy and users' electricity cost. Liu et al. [39] propose a consensus-based distributed speed advisory system that optimally determines a common vehicle speed for a given area in a privacy-aware manner to minimize the total emission of fuel vehicles or the total energy consumption of EVs. Other applications can be found in data mining [40], cloud computing [41], etc. To the best of our knowledge, this work is the first to discuss the distributed scheduling of EV battery swapping in light of binary station assignments and microgrid operation.

2 Problem formulation

We focus on the scenario where a fleet of EVs and a set of service stations operate in a region that is supplied by a microgrid. We assume the microgrid, service stations, and EVs are managed centrally by the same operator, for example, the State Grid in China. Periodically, say, every 15 min, the system determines a set of EVs that should be scheduled for battery swapping, for example, based on their current states of charge or their requests for battery swapping. At the beginning of the current control interval, the system assigns to each EV in the set a service station for battery swapping. It is reasonable

to assume that the EVs travel to their assigned service stations and finish swapping their batteries before the end of the current interval, since typically the geographic area served by a microgrid is limited. Under this assumption, station assignments are decoupled across control intervals and our work focuses on one such interval.

Batteries returned by the EVs start to be charged at the service stations immediately (typically at service stations each battery is placed in a charging box before being swapped, thus a returned battery can immediately find its place in a charging box). Since we focus on the scheduling of battery swapping, we assume for simplicity that these batteries are charged at the constant rated power for the control interval under study, which contributes to better serving future battery swapping demand as well. Optimizing charging rates over multiple intervals can be integrated with battery swapping if more future information is available, but that is beyond the scope of the current work. Our goal is to design an assignment algorithm that minimizes a weighted sum of the distance traveled by the EVs for battery swapping and electricity generation cost, while respecting the EVs' range constraints, the operational constraints of the microgrid, and AC power flow equations.

In the following we formulate our optimal scheduling problem. For a finite set $\mathbb{K}$ that consists of some natural numbers, its cardinality is denoted as $|\mathbb{K}|$. For a set of scalar variables y_j, $j \in \mathbb{K}$, its column vector is denoted as $y_{\mathbb{K}}$. $y_{\mathbb{K}}^T$ and $y_{\mathbb{K}}^H$ denote its transpose and Hermitian transpose, respectively. Sometimes the subscript $\mathbb{K}$ is dropped if the set is clear from the context. For a matrix Y, Y^T and Y^H denote its transpose and Hermitian transpose, respectively. Let $Y_{i,j}$ be the (i,j)th element of Y and $Y_{\mathbb{K}_1\mathbb{K}_2}$ be a submatrix of Y composed of all the element Y_{ij}, $i \in \mathbb{K}_1$ and $j \in \mathbb{K}_2$.

2.1 Network model

Consider a single-phase microgrid network with a connected directed graph $\mathbb{G} = (\mathbb{N}, \mathbb{E})$, where $\mathbb{N} := \{0, 1, 2, \ldots, N\}$ and $\mathbb{E} \subseteq \mathbb{N} \times \mathbb{N}$. Each node in $\mathbb{N}$ represents a bus and each edge in $\mathbb{E}$ represents a power line. Let $\mathbb{N}^+ := \{1, 2, \ldots, N\}$. Bus 0 is a slack bus if $\mathbb{G}$ is a mesh network, or a root bus if $\mathbb{G}$ is a radial (tree) network. We orient the graph, without loss of generality, by denoting a line in $\mathbb{E}$ by (j,k) or $j \to k$ if it points from bus j to bus k. Let z_{jk} be the complex impedance of line $(j,k) \in \mathbb{E}$, and $y_{jk} = \frac{1}{z_{jk}}$ be the corresponding complex admittance. Let $S_{jk} := P_{jk} + \mathbf{i}Q_{jk}$ denote the *sending-end* complex power from bus j to bus k where P_{jk} and Q_{jk} denote the real and reactive power flows, respectively. Define I_{jk} as the complex current from bus j to bus k and V_j as the complex voltage phasor of bus j with its angle denoted by θ_j. Assume the voltage V_0 of bus 0 is fixed and given.

Each bus j has a base load $s_j^b := p_j^b + \mathbf{i}q_j^b$ (excluding the charging loads from stations), where p_j^b and q_j^b denote the real and reactive power, respectively.

Each bus j may also have distributed generation $s_j^g := p_j^g + \mathbf{i}q_j^g$. Let $s_j := p_j + \mathbf{i}q_j$ denote the net complex power injection given by

$$s_j := \begin{cases} s_j^g - s_j^b - s_j^e & \text{if bus } j \text{ supplies a station} \\ s_j^g - s_j^b & \text{otherwise} \end{cases}$$

where s_j^e denotes the total charging load at bus j. We assume the base loads s_j^b are given and the generations s_j^g and charging loads s_j^e are variables.

We then summarize three representative linearization/convexification methods to model the power flows on the microgrid that are useful depending on network topologies and parameterization.

2.1.1 DC power flow equations

Assumptions:

1. The bus voltage magnitude is constant as 1.
2. Each line is lossless.
3. Reactive power injections and flow are ignored.
4. The bus phase angle difference across each line is small.

Given these standard assumptions for DC approximation, the generic AC power flow equations reduce to

$$\sum_{k:(j,k)\in\mathbb{E}} P_{jk} = \sum_{k:(i,j)\in\mathbb{E}} P_{ij} + p_j, \quad j \in \mathbb{N} \tag{1a}$$

$$P_{jk} = B_{jk}(\theta_j - \theta_k), \quad j \to k \in \mathbb{E} \tag{1b}$$

where B_{jk} is the negative susceptance of line (j,k). Eq. (1a) enforces nodal power balance while Eq. (1b) defines line flows. This is the simplest linear model of power flows and it applies to systems where (a) the line resistance is negligible, and for normal operating points, (b) the bus phase angle difference across each line is small, and (c) the bus voltage magnitude is very close to 1 in the per-unit system.

The complex notation of Eq. (1) is only a shorthand for a set of real equations in the real vector variables $(p, P, \theta) := (p_j, P_{jk}, \theta_j, j, k \in \mathbb{N}, (j,k) \in \mathbb{E})$.

2.1.2 Fix-point linearization of power flow equations

Let $\hat{I}_{\mathbb{N}^+} := (\hat{I}_j, j \in \mathbb{N}^+)$ be the vector of net current injections at all buses $j \in \mathbb{N}^+$. The bus injection model of power flows can be written as

$$\hat{I}_{\mathbb{N}^+} = Y_{\mathbb{N}^+0} V_0 + Y_{\mathbb{N}^+\mathbb{N}^+} V_{\mathbb{N}^+} \tag{2a}$$

$$_{\mathbb{N}^+} = \text{diag}(V_{\mathbb{N}^+})\hat{I}^H_{\mathbb{N}^+} \tag{2b}$$

where Y is the admittance matrix of the microgrid with $Y_{ij} = -y_{ij}$ if $i \neq j$ and $Y_{ii} = \sum_{j\neq i} y_{ij}$ if $i = j$. Eq. (2a) imposes nodal balance of current (power)

while Eq. (2b) defines bus power injections. Substituting Eq. (2b) into Eq. (2a) to eliminate $\hat{I}_{\mathbb{N}^+}$, we can attain the following fixed-point equation:

$$V_{\mathbb{N}^+} = -Y_{\mathbb{N}^+\mathbb{N}^+}^{-1} Y_{\mathbb{N}^+0} V_0 + Y_{\mathbb{N}^+\mathbb{N}^+}^{-1} \mathrm{diag}^{-1}(V_{\mathbb{N}^+}^H) s_{\mathbb{N}^+}^H \tag{3}$$

where the first term is a constant vector meaning *zero-load voltage*.

Given a nominal operation point $(\hat{V}_{\mathbb{N}^+}, \hat{s}_{\mathbb{N}^+})$ that is a solution to Eq. (3), we are able to linearize Eq. (2) in the following linear form based on one single iteration of Eq. (3):

$$V_{\mathbb{N}^+} = J[p_{\mathbb{N}^+}^T, q_{\mathbb{N}^+}^T]^T + a \tag{4a}$$

where $J := [Y_{\mathbb{N}^+\mathbb{N}^+}^{-1} \mathrm{diag}^{-1}(\hat{V}_{\mathbb{N}^+}^H), -\mathbf{i} Y_{\mathbb{N}^+\mathbb{N}^+}^{-1} \mathrm{diag}^{-1}(\hat{V}_{\mathbb{N}^+}^H)]$ and $a := -Y_{\mathbb{N}^+\mathbb{N}^+}^{-1} Y_{\mathbb{N}^+0} V_0$. Let $I := (I_{jk}, (j,k) \in \mathbb{E})$. It follows from [42] that $|V_{\mathbb{N}^+}|$ and I can also be linearly approximated in terms of $[p_{\mathbb{N}^+}^T, q_{\mathbb{N}^+}^T]^T$:

$$|V_{\mathbb{N}^+}| = K[p_{\mathbb{N}^+}^T, q_{\mathbb{N}^+}^T]^T + b \tag{4b}$$

$$I = L[p_{\mathbb{N}^+}^T, q_{\mathbb{N}^+}^T]^T + c \tag{4c}$$

$$s_0 = D[p_{\mathbb{N}^+}^T, q_{\mathbb{N}^+}^T]^T + d \tag{4d}$$

where K, L, D are also constant matrices dependent on $\hat{V}_{\mathbb{N}^+}$ and b, c, d are constant vectors. We refer readers to [42] for the detailed derivation and expressions of these parameters.

The fixed-point linearization of power flow Eq. (4) interpolates between two power flow solutions $(\hat{V}_{\mathbb{N}^+}, \hat{s}_{\mathbb{N}^+})$ and $(a, 0)$, and is more computationally affordable than a lot of classical methods, for example, the first-order Taylor method. In most cases it also provides a better global approximation.

The complex notation of Eq. (4) is only a shorthand for a set of real equations in the real vector variables $(s, V, |V|, I) := (p, q, V, |V|, I) := (p_j, q_j, V_j, |V_j|, I_{jk}, j, k \in \mathbb{N}, (j,k) \in \mathbb{E})$.

2.1.3 DistFlow equations and SOCP relaxation

Suppose the microgrid is a radial network; the unique parent bus of each bus j (except bus 0) is indexed by $i := i_j$. Define $l_{jk} := |I_{jk}|^2$ as the squared magnitude of the complex current from bus j to bus k and $v_j := |V_j|^2$ as the squared magnitude of the complex voltage phasor of bus j.

We use the *DistFlow* equations proposed by Baran and Wu in [43] to model power flows on the network:

$$\sum_{k:(j,k)\in\mathbb{E}} S_{jk} = S_{ij} - z_{ij} l_{ij} + s_j, \quad j \in \mathbb{N} \tag{5a}$$

$$v_j - v_k = 2\mathrm{Re}(z_{jk}^H S_{jk}) - |z_{jk}|^2 l_{jk}, \quad j \to k \in \mathbb{E} \tag{5b}$$

$$v_j l_{jk} = |S_{jk}|^2, \quad j \to k \in \mathbb{E} \tag{5c}$$

The equations impose power balance at each bus in Eq. (5a), model the Ohm's law in Eq. (5b), and define branch power flows in Eq. (5c). Note that $S_{i0} := 0$ and $l_{i0} := 0$ when bus $j = 0$ is the root bus, and when bus j is a leaf node of $\mathbb{G}$, all $S_{jk} = 0$ in Eq. (5a). The quantity $z_{ij}l_{ij}$ is the loss on line (i,j), and hence $S_{ij} - z_{ij}l_{ij}$ is the *receiving-end* complex power at bus j from bus i.

With the definition of v and l, Eqs. (5a), (5b) are both linear in variables. However, the *DistFlow* equations are still difficult to solve due to the nonconvex quadratic equality (5c). To deal with this nonconvexity, we adopt the recently developed second-order cone programming (SOCP) relaxation. Note that by relaxing the quadratic equality into inequality, that is,

$$v_j l_{jk} \geq |S_{jk}|^2 \longleftrightarrow \left\| \begin{array}{c} 2P_{jk} \\ 2Q_{jk} \\ v_j - l_{jk} \end{array} \right\|_2 \leq v_j + l_{jk}, \quad j \to k \in \mathbb{E}$$

the nonconvex constraint (5c) is relaxed into a second-order cone. Specifically, we have the relaxed convex *DistFlow* equations:

$$\sum_{k:(j,k)\in\mathbb{E}} S_{jk} = S_{ij} - z_{ij}l_{ij} + s_j, \quad j \in \mathbb{N} \tag{6a}$$

$$v_j - v_k = 2\mathrm{Re}(z_{jk}^H S_{jk}) - |z_{jk}|^2 l_{jk}, \quad j \to k \in \mathbb{E} \tag{6b}$$

$$v_j l_{jk} \geq |S_{jk}|^2, \quad j \to k \in \mathbb{E} \tag{6c}$$

When we solve an OPF problem that satisfies Eq. (5), an alternative is to look at its relaxation with Eq. (6) replacing Eq. (5). If an optimal solution to the relaxation attains equality in Eq. (6c), then the solution is also feasible, and therefore *optimal*, for the original OPF problem. In this case, we say the SOCP relaxation is *exact*. Sufficient conditions are known that guarantee the exactness of the SOCP relaxation; see Refs. [44, 45] for a comprehensive tutorial and references therein. Even when these conditions are not satisfied, the SOCP relaxation for practical radial networks is still often exact, as confirmed also by our simulations in Section 5. Therefore, Eq. (6) is a computationally tractable power flow model for radial networks by assuming the underlying SOCP relaxation is exact.

The complex notation of Eq. (6) is only a shorthand for a set of real equations in the real vector variables $(s, v, l, S) := (p, q, v, l, P, Q) := (p_j, q_j, v_j, l_{jk}, P_{jk}, Q_{jk}, j, k \in \mathbb{N}, (j,k) \in \mathbb{E})$.

2.1.4 Operational constraints

The operation of the microgrid must meet certain specifications. The voltage magnitudes must be maintained within stable regions:

$$\underline{V}_j \leq |V_j| \leq \overline{V}_j \quad \text{or} \quad \underline{v}_j \leq v_j \leq \overline{v}_j, \qquad j \in \mathbb{N} \tag{7a}$$

where $\underline{V}_j$, $\underline{v}_j$ and $\overline{V}_j$, $\overline{v}_j$ are given lower and upper bounds on the (squared) voltage magnitude at bus j, respectively. The distributed real and reactive generations must satisfy

$$\underline{p}_j^g \le p_j^g \le \overline{p}_j^g, \quad j \in \mathbb{N} \tag{7b}$$

$$\underline{q}_j^g \le q_j^g \le \overline{q}_j^g, \quad j \in \mathbb{N} \tag{7c}$$

where $\underline{p}_j^g, \overline{p}_j^g$ and $\underline{q}_j^g, \overline{q}_j^g$ are given lower and upper bounds on the real and reactive power generations at bus j, respectively. The thermal limit of line (j,k) must be satisfied:

$$P_{jk} \le \overline{P}_{jk}, \text{ or } |I_{jk}| \le \overline{I}_{jk}, \text{ or } |S_{jk}| \le \overline{S}_{jk}, \quad j \to k \in \mathbb{E} \tag{7d}$$

where $\overline{P}_{jk}, \overline{I}_{jk}$, and $\overline{S}_{jk}$ denote different representations of the thermal limit of line (j,k).

The model is quite general. If a quantity is known and fixed, then we set both its upper and lower bounds to the given quantity, for example, the voltage of the substation bus. If there is no distributed generation at bus j, then $\overline{p}_j^g = \underline{p}_j^g = \overline{q}_j^g = \underline{q}_j^g = 0$.

2.2 Battery swapping scheduling

Let $\mathbb{N}_w := \{1, 2, \ldots, N_w\} \subseteq \mathbb{N}$ denote the set of buses that supply electricity to stations, whose locations are fixed and known. For simplicity, assume there is only one station (or an ensemble of multiple stations) connected to each bus $j \in \mathbb{N}_w$ and we use j to index both the bus and the station. The batteries at each station are either charging at the constant rated power r or already fully charged and ready for swapping. Denote the total numbers of batteries and fully charged batteries at station j at the beginning of the current control interval by M_j and m_j, respectively. Note that M_j is always fixed while m_j is observed in each interval.

Let $\mathbb{A} := \{1, 2, \ldots, A\}$ denote the set of EVs in the service area that require battery swapping in the current interval. Denote their states of charge as $(c_a, a \in \mathbb{A})$. Let u_{aj} represent the assignment:

$$u_{aj} = \begin{cases} 1, & \text{if station } j \text{ is assigned to EV } a \\ 0, & \text{otherwise} \end{cases}$$

and let $u := (u_{aj},\ a \in \mathbb{A}, j \in \mathbb{N}_w)$ denote the vector of assignments.

The assignments u satisfy the following conditions:

$$\sum_{j \in \mathbb{N}_w} u_{aj} = 1, \quad a \in \mathbb{A} \tag{8a}$$

$$\sum_{a \in \mathbb{A}} u_{aj} \le m_j, \quad j \in \mathbb{N}_w \tag{8b}$$

that is, exactly one station is assigned to every EV and every assigned station has enough fully charged batteries.

The system knows the current location of every EV a and therefore can calculate the distance d_{aj} from its current location to the assigned station j, for example, by resorting to a routing application (like Google Maps). In the electric taxi case, if EV a is not currently carrying passengers and can go to swap its battery immediately, then d_{aj} is the travel distance from its current location to station j. If EV a must first complete its current passenger run before going to station j, then d_{aj} is the travel distance from its current location to the destination of its passengers and then to station j. The assigned station j must be within each EV a's driving range, that is,

$$u_{aj}d_{aj} \le \gamma_a c_a, \quad j \in \mathbb{N}_w, a \in \mathbb{A} \tag{8c}$$

where c_a is EV a's current state of charge and γ_a is its driving range per unit state of charge.

Denote the constraint set for u by

$$\mathbb{U} := \{u \in \{0,1\}^{AN_w} : u \text{ satisfies Eq. (8)}\}$$

Assumption 1. $\mathbb{U}$ is nonempty.

Under Assumption 1, there are enough fully charged batteries in the system for all EVs in $\mathbb{A}$ in the current interval. This can be enforced when choosing the candidate set $\mathbb{A}$ of EVs for battery swapping, for example, for EVs that can reach the same subset of stations, ranking them according to their states of charge, scheduling as many EVs as possible in an increasing order, upper limited by the number of fully charged batteries at those stations, and postponing remaining EVs to the next interval.

Since every EV produces a depleted battery that needs to be charged at the rated power r, we can express the net power injection $s_j = p_j + \mathbf{i}q_j$ at bus j in terms of the assignments u as

$$p_j = \begin{cases} p_j^g - p_j^b - r\left(M_j - m_j + \sum_{a\in\mathbb{A}} u_{aj}\right), & j \in \mathbb{N}_w \\ p_j^g - p_j^b, & j \in \mathbb{N} \setminus \mathbb{N}_w \end{cases} \tag{9a}$$

$$q_j = q_j^g - q_j^b, \quad j \in \mathbb{N} \tag{9b}$$

Let $f_j\colon \mathbb{R} \to \mathbb{R}$ model the generation cost at bus j, for example, for a distributed gas generator. We assume all f_js are increasing and convex functions, for example, quadratic functions [17–19]. Denote the power flow variables by ϕ. Given the previous three network models, $\phi \in \{(p, P, \theta), (s, V, |V|, I), (s, v, l, S)\}$, and corresponds to the model used. We are interested in the following optimization problem:

$$\min_{u, s^g, \phi} \sum_{j\in\mathbb{N}} f_j(p_j^g) + \alpha \sum_{a\in\mathbb{A}} \sum_{j\in\mathbb{N}_w} d_{aj}u_{aj} \tag{10}$$

$$\text{s.t.} \quad \text{Eq. (1) or (4) or Eqs. (6)–(9)}, \quad u \in \{0,1\}^{AN_w}$$

where $\sum_{a\in\mathbb{A}}\sum_{j\in\mathbb{N}_w} u_{aj}d_{aj}$ is the total travel distance of EVs and $\alpha > 0$ is a weight that makes electricity generation cost and travel distance comparable, for example, the travel cost per unit of distance. The network model can be properly chosen based on the topologies and parameterization of the microgrid. Fixing any assignments $u \in \{0,1\}^{AN_w}$, the problem (10) is a convex problem.

3 Centralized solution

The joint battery swapping and OPF problem (10) is generally difficult to solve because the assignments u are discrete. Our centralized solution applies generalized Benders decomposition to deal with the discrete variables in Eq. (10). Benders decomposition was first proposed in [46] for problems where, when a subset of the variables are fixed, the remaining subproblem is a linear program. It is extended in [47] to problems where the remaining subproblem is a convex program. We now apply it to solving Eq. (10).

Denote the continuous variables by $x := (s^g, \phi)$ while the discrete variables are u. Denote the objective function by

$$F(x,u) := \sum_{j\in\mathbb{N}} f_j(p_j^g) + \alpha \sum_{a\in\mathbb{A}}\sum_{j\in\mathbb{N}_w} d_{aj}u_{aj}$$

Given any u, $F(x,u)$ is convex in x since f_js are assumed to be strictly convex. Denote the constraint set for x by

$$\mathbb{X} := \{x \in \mathbb{R}^{(|\mathbb{N}|+|\phi|)} : x \text{ satisfies Eq. (7) and one of Eq. (1), (4) or (6)}\}$$

and the constraints (9) on (x,u) by $G(x,u) = 0$ while $u \in \mathbb{U}$. Then the relaxation (10) takes the standard form for generalized Benders decomposition:

$$\begin{aligned} &\min_{x,u} \; F(x,u) \\ &\text{s.t.} \quad G(x,u) = 0, \quad x \in \mathbb{X}, \; u \in \mathbb{U} \end{aligned} \tag{11}$$

where F: $\mathbb{R}^{(|\mathbb{N}|+|\phi|)} \times \{0,1\}^{AN_w} \to \mathbb{R}$ is a scalar-valued function, and G: $\mathbb{R}^{(|\mathbb{N}|+|\phi|)} \times \{0,1\}^{AN_w} \to \mathbb{R}^{2|\mathbb{N}|}$ is a vector-valued constraint function. Fixing any $u \in \mathbb{U}$, Eq. (11) is a convex subproblem in x. We now apply generalized Benders decomposition of [47] to Eq. (11).

Write Eq. (11) in the following equivalent form:

$$\min_{u} \; W(u) \quad \text{s.t.} \quad u \in \mathbb{U} \cap \mathbb{W} \tag{12a}$$

where, for a fixed value of u,

$$\begin{aligned} W(u) := \; &\min_{x\in\mathbb{X}} \quad F(x,u) \\ &\text{s.t.} \quad G(x,u) = 0 \end{aligned} \tag{12b}$$

and

$$\mathbb{W} := \{u : G(x,u) = 0 \quad \text{for some } x \in \mathbb{X}\} \tag{12c}$$

The problem (12b), called the slave problem, is convex and much easier to solve than Eq. (11). The set $\mathbb{W}$ consists of all us for which Eq. (12b) is feasible and hence $\mathbb{U} \cap \mathbb{W}$ is the projection of the feasible region of Eq. (11) onto the u-space. The central idea of generalized Benders decomposition is to invoke the dual representations of $W(u)$ and $\mathbb{W}$ to derive the following equivalent problem to Eq. (12) (see [47, Theorems 2.2 and 2.3]):

$$\min_{u\in\mathbb{U}} \sup_{\mu\in\mathbb{R}^{2|\mathbb{N}|}} \left\{ \min_{x\in\mathbb{X}} \left\{ F(x,u) + \mu^T G(x,u) \right\} \right\}$$
$$\text{s.t.} \min_{x\in\mathbb{X}} \left\{ \lambda^T G(x,u) \right\} = 0, \quad \forall \lambda \in \mathbb{R}^{2|\mathbb{N}|}$$

Note that we assume that Slater's condition is always satisfied. Here λ and μ are Lagrangian multiplier vectors for $\mathbb{W}$ and $W(u)$, respectively. This problem is equivalent to

$$\min_{u\in\mathbb{U}, u_0\in\mathbb{R}} u_0 \tag{13}$$
$$\text{s.t.} \quad u_0 \geq \min_{x\in\mathbb{X}} \left\{ F(x,u) + \mu^T G(x,u) \right\}, \quad \forall \mu \in \mathbb{R}^{2|\mathbb{N}|}$$
$$\min_{x\in\mathbb{X}} \left\{ \lambda^T G(x,u) \right\} = 0, \quad \forall \lambda \in \mathbb{R}^{2|\mathbb{N}|}$$

In summary, the series of manipulations have transformed the relaxation (10) into the master problem (13).

Since Eq. (13) has uncountably many constraints with all possible λs and μs, it is neither practical nor necessary to enumerate all constraints in solving Eq. (13). Generalized Benders decomposition starts by solving a relaxed version of Eq. (13) that ignores all but a few constraints. If a solution to the relaxed version of Eq. (13) satisfies all the ignored constraints, then it is an optimal solution to Eq. (13) and the algorithm terminates. Otherwise, the solution process of the relaxed version of Eq. (13) will identify one μ or λ for which the corresponding constraint is violated. The violated constraint is then added to the relaxed version of Eq. (13), and the cycle repeats.

Specifically, the generalized Benders decomposition algorithm for Eq. (10) (or equivalently, Eq. 11) is as follows.

- *Step 1.* Pick any $\bar{u} \in \mathbb{U} \cap \mathbb{W}$. Solve the dual problem of Eq. (12b) with $u = \bar{u}$ to obtain an optimal Lagrangian multiplier vector $\bar{\mu}$. Let $n_\mu = 1$, $n_\lambda = 0$, $\mu^1 = \bar{\mu}$, and $UBD = W(\bar{u})$, where n_μ, n_λ are counters for the two types of constraints in Eq. (13), and *UBD* denotes an upper bound on the optimal value of Eq. (11).

- *Step 2.* Solve the current relaxed master problem:

$$\begin{aligned} &\min_{u\in\mathbb{U},u_0\in\mathbb{R}} u_0 \\ &\text{s.t.} \quad u_0 \geq \min_{x\in\mathbb{X}} \left\{F(x,u) + \left(\mu^i\right)^T G(x,u)\right\}, \quad i = 1,\ldots,n_\mu \\ &\min_{x\in\mathbb{X}} \left\{\left(\lambda^i\right)^T G(x,u)\right\} = 0, \quad i = 1,\ldots,n_\lambda \end{aligned} \tag{14}$$

  Let $(\hat{u},\hat{u}_0)$ be the optimal solution to Eq. (14). Clearly $\hat{u}_0$ is a lower bound on the optimal value of Eq. (11) since the constraints in Eq. (13) are relaxed to a smaller set of constraints in Eq. (14). Terminate the algorithm if $UBD - \hat{u}_0 \leq \epsilon$, where $\epsilon > 0$ is a sufficiently small threshold.
- *Step 3.* Solve the dual problem of Eq. (12b) with $u = \hat{u}$. The solution falls into the following two cases.

  1. *Step 3a. The dual problem of Eq. (12b) has a bounded solution* $\hat{\mu}$, that is, $W(\hat{u})$ is feasible and finite. Let $UBD = \min\{UBD, W(\hat{u})\}$. Terminate the algorithm if $UBD - \hat{u}_0 \leq \epsilon$. Otherwise, increase n_μ by 1 and let $\mu^{n_\mu} = \hat{\mu}$. Return to *Step 2*.
  2. *Step 3b. The dual problem of Eq. (12b) has an unbounded solution*, that is, $W(\hat{u})$ is infeasible. Determine $\hat{\lambda}$ through a feasibility check problem and its dual [48]. Increase n_λ by 1 and let $\lambda^{n_\lambda} = \hat{\lambda}$. Return to *Step 2*.

We make three remarks. First, the slave problem (12b) is convex and hence can generally be solved efficiently. The relaxed master problem (14) involves discrete variables and is generally nonconvex, but it is much simpler than the original problem (11). Second, for our problem, Eq. (14) turns out to be a mixed-integer linear program in essence because both F and G are separable functions in (x,u) of the form

$$\begin{aligned} F(x,u) &=: F_1(x) + F_2(u) \\ G(x,u) &=: G_1(x) + G_2(u) \end{aligned}$$

where F_2 and G_2 are both linear in u. Indeed the constraints in Eq. (14) are

$$\begin{aligned} u_0 - F_2(u) - \left(\mu^i\right)^T G_2(u) &\geq \min_{x\in\mathbb{X}} \left\{F_1(x) + \left(\mu^i\right)^T G_1(x)\right\}, \quad i = 1,\ldots,n_\mu \\ \left(\lambda^i\right)^T G_2(u) &= -\min_{x\in\mathbb{X}} \left(\lambda^i\right)^T G_1(x), \quad i = 1,\ldots,n_\lambda \end{aligned}$$

where the left-hand side is linear in u and the right-hand side is independent of u. Hence, in each iteration, the algorithm solves Eq. (14), which is a simplified mixed-integer linear program (always with only one continuous auxiliary variable), and Eq. (12b), which is a convex program. Third, every time Step 2 is entered, one additional constraint is added to Eq. (14). This generally makes Eq. (14) harder to compute, but also a better approximation of Eq. (13). It is proved in [47, Theorem 2.4] that the algorithm will terminate in finite steps since $\mathbb{U}$ is discrete and finite.

4 Distributed solutions

4.1 Relaxations

The joint battery swapping and OPF problem (10) is computationally difficult since the assignment variables u are binary. To deal with this difficulty, we use generalized Benders decomposition in Section 3. This approach could compute an optimal solution in reasonable time but the computation is centralized and is suitable only when a single organization, for example, the State Grid in China, operates all of the microgrid, stations, and EVs. This section develops distributed solutions that are suitable for systems where these three are operated by separate entities that do not share their private information. To this end, we relax the binary assignment variables u to real variables $u \in [0,1]^{AN_w}$. The constraints (8) are then replaced by

$$u_{aj} = 0 \quad \text{if } d_{aj} > \gamma_a c_a, \quad j \in \mathbb{N}_w,\ a \in \mathbb{A} \tag{15a}$$

$$\sum_{j \in \mathbb{N}_w} u_{aj} = 1, \quad a \in \mathbb{A} \tag{15b}$$

$$\sum_{a \in \mathbb{A}} u_{aj} \le m_j, \quad j \in \mathbb{N}_w \tag{15c}$$

and we change to solve the following relaxation of Eq. (10):

$$\min_{u, s^g, \phi} \sum_{j \in \mathbb{N}} f_j(p_j^g) + \alpha \sum_{a \in \mathbb{A}} \sum_{j \in \mathbb{N}_w} d_{aj} u_{aj} \tag{16}$$

$$\text{s.t.} \quad \text{Eq. (1) or (4) or (6), (7), (9), (15)}, \quad u \in \{0,1\}^{AN_w}$$

This problem has a convex objective and convex quadratic constraints. After an optimal solution (x^*, u^*) to Eq. (16) is obtained, we discretize u^*_{aj} into $\{0,1\}$, for example, by setting for each EV a a single large u^*_{aj} to 1 and the rest to 0 heuristically. An alternative is to randomize the station assignments using u^* as a probability distribution. Whichever method is employed, it should guarantee the discretized station assignments are feasible. As we will show later, the discretization is readily implementable and achieves binary station assignments close to optimum.

4.2 Distributed solution via ADMM

The relaxation (16) decomposes naturally into two subproblems, one on station assignments over u and the other on OPF over (s^g, ϕ). The station assignment subproblem will be solved by a station operator that operates the network of stations. The OPF subproblem will be solved by a utility company. Our goal is to design a distributed algorithm for them to solve jointly Eq. (16) without sharing their private information.

These two subproblems are coupled only in Eq. (9a) where the utility company needs the charging load $s_j^e = r\left(M_j - m_j + \sum_{a\in\mathbb{A}} u_{aj}\right)$ of station j in order to compute the net real power injection p_j. This quantity depends on the total number of EVs that each station j is assigned to and is computed by the station operator. Their computation can be decoupled by introducing an auxiliary variable w_j at each bus (station) j that represents the utility company's estimate of the quantity $r\left(M_j - m_j + \sum_{a\in\mathbb{A}} u_{aj}\right)$, and requiring that they be equal at optimality.

Specifically, recall the station assignment variables u, and denote the power flow variables by $x := (w, s^g, \phi)$ where $w := \left(r\left(M_j - m_j + \sum_{a\in\mathbb{A}} u_{aj}\right), j \in \mathbb{N}_w\right)$. Separate the objective function by defining

$$f(x) := \sum_{j\in\mathbb{N}} f_j(p_j^g)$$

$$g(u) := \alpha \sum_{a\in\mathbb{A}} \sum_{j\in\mathbb{N}_w} d_{aj} u_{aj}$$

Replace the coupling constraints (9) by constraints local to bus j:

$$p_j = \begin{cases} p_j^g - p_j^b - w_j, & j \in \mathbb{N}_w \\ p_j^g - p_j^b, & j \in \mathbb{N}/\mathbb{N}_w \end{cases} \tag{17a}$$

$$q_j = q_j^g - q_j^b, \quad j \in \mathbb{N} \tag{17b}$$

Denote the local constraint set for x by

$$\mathbb{X} := \left\{ x \in \mathbb{R}^{(|\mathbb{N}_w|+|\mathbb{N}|+|\phi|)} : x \text{ satisfies Eqs. (7), (17) and one of Eq. (1), (4) or (6)} \right\}$$

Denote the local constraint set for u by

$$\mathbb{U} := \left\{ u \in \mathbb{R}^{AN_w} : u \text{ satisfies Eq. (15)} \right\}$$

To simplify the notation, define $u_j := \sum_{a\in\mathbb{A}} u_{aj}$ for $j \in \mathbb{N}_w$. Then the relaxation (16) is equivalent to

$$\min_{x,u} \quad f(x) + g(u) \tag{18a}$$

$$\text{s.t.} \quad x \in \mathbb{X},\ u \in \mathbb{U} \tag{18b}$$

$$w_j = r\left(M_j - m_j + u_j\right), \quad j \in \mathbb{N}_w \tag{18c}$$

We now apply ADMM to Eq. (18). Let $\lambda := (\lambda_j, j \in \mathbb{N}_w)$ be the Lagrange multiplier vector corresponding to the current coupling constraint (18c), and define the augmented Lagrangian:

$$L_\rho(x, u, \lambda) := f(x) + g(u) + h_\rho(w, u, \lambda) \tag{19a}$$

where h_ρ depends on (x, u) only through $(w_j, u_j, j \in \mathbb{N}_w)$:

$$h_\rho(w, u, \lambda) := \sum_{j\in\mathbb{N}_w} \lambda_j[w_j - r\left(M_j - m_j + u_j\right)] + \frac{\rho}{2} \sum_{j\in\mathbb{N}_w} [w_j - r\left(M_j - m_j + u_j\right)]^2 \tag{19b}$$

and ρ is the step size for dual variable λ updates. The standard ADMM procedure is iteratively and sequentially to update (x, u, λ): for $n = 0, 1, \ldots,$

$$x(n+1) := \arg\min_{x\in\mathbb{X}} f(x) + h_\rho(w, u(n), \lambda(n)) \tag{20a}$$

$$u(n+1) := \arg\min_{u\in\mathbb{U}} g(u) + h_\rho(w(n+1), u, \lambda(n)) \tag{20b}$$

$$\lambda_j(n+1) := \lambda_j(n) + \rho[w_j(n+1) - r(M_j - m_j + u_j(n+1))], \quad j \in \mathbb{N}_w \tag{20c}$$

Remark 1.

1. The x-update (20a) is carried out by the utility company and involves minimizing a convex objective with convex quadratic constraints. The (u, λ)-updates (20b), (20c) are carried out by the station operator and the u-update minimizes a convex quadratic objective with linear constraints. Both can be efficiently solved.
2. The x-update by the utility company in iteration $n + 1$ needs $(u(n), \lambda(n))$ from the station operator. From Eq. (19b), the station operator does not need to communicate the detailed assignments $u(n) = (u_{aj}(n),\ a \in \mathbb{A},\ j \in \mathbb{N}_w)$ to the utility company, but only the charging load $s_j^e = r(M_j - m_j + u_j(n))$ of each station j.
3. The (u, λ)-updates by the station operator in iteration $n + 1$ need the utility company's estimate $w(n + 1)$ of $(r(M_j - m_j + u_j(n + 1)), j \in \mathbb{N}_w)$.
4. The reason why the x-update by the utility company needs $(u_j(n), j \in \mathbb{N}_w)$ and the u-update by the station operator needs $w(n + 1)$ lies in the (quadratic) regularization term in h_ρ. This becomes unnecessary for the dual decomposition approach in Section 4.3 without the regularization term.

The communication structure is illustrated in Fig. 2. In particular, private information of the utility company, such as network parameters $(z_{jk}, (j, k) \in \mathbb{E})$, network states $(s^g(n), \phi(n))$, cost functions f, and operational constraints, as well as private information of the station operator, such as the total numbers of batteries $(M_j, j \in \mathbb{N}_w)$, the numbers of available fully charged batteries $(m_j, j \in \mathbb{N}_w)$, how many EVs or where they are or their states of charge, and the detailed assignments $u(n)$, does not need to be communicated.

When the cost functions f_j are closed, proper, and convex, and $L_\rho(x, u, \lambda)$ has a saddle point, the ADMM iteration (20) converges in that, for any $j \in \mathbb{N}_w$, the mismatch $|w_j(n) - r(M_j - m_j + u_j(n))| \to 0$ and the objective function $f(x(n)) + g(u(n))$ converges to its minimum value [49]. This does not automatically guarantee that $(x(n), u(n))$ converges to an optimal solution

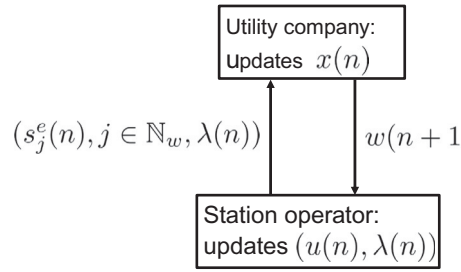

Fig. 2 Communication between utility company and station operator.

to Eq. (16). In theory, ADMM may converge and circulate around the set of optimal solutions, but never reach one. In practice, a solution within a given error tolerance is acceptable. If $(x(n), u(n))$ indeed converges to a primal optimal solution (x^*, u^*), u^* may generally not be binary. We can use a heuristic to derive binary station assignments from u^*, as mentioned earlier. Fortunately, the following result shows that the number of EVs with nonbinary assignments is bounded and small in u^*. See Appendix for its proof.

Theorem 1. *It is always possible to find an optimal solution* (x^*, u^*) *to the relaxation (16) in which the number of EVs a with* $u^*_{aj} < 1$ *for any* $j \in \mathbb{N}_w$ *is at most* $N_w(N_w - 1)/2$.

In practice, the number N_w of stations is much smaller than the number A of EVs that request battery swapping, and hence the number of nonbinary assignments that need to be discretized will be small. Simulations in Section 5 further suggest that the discretized assignments are close to optimum.

4.3 Distributed solution via dual decomposition

The ADMM-based solution assumes the station operator directly controls the station assignments to all EVs. This requires that the station operator know the locations (d_{aj}), states of charge (c_a), and performance (γ_a) of EVs. Moreover, the charging load $s_j^e = r(M_j - m_j + u_j(n))$ of each station j needs to be provided to the utility company. We now present another solution based on dual decomposition that is more suitable in situations where it is undesirable or inconvenient to share private information between the utility company, the station operator, and EVs.

In the original relaxation (16), the update of the net power injections p_j in Eq. (9) by the utility company involves u_j which is updated by the station operator. These two computations are decoupled in the ADMM-based solution by introducing an auxiliary variable w_j for each $j \in \mathbb{N}_w$ at the utility company and relaxing the constraint $w_j = r(M_j - m_j + u_j)$. In addition, the station assignments u must satisfy $u_j \le m_j$ in Eq. (15c). This is enforced in the ADMM-based solution by the station operator that computes u for all EVs. To distribute fully the computation to individual EVs, we dualize $u_j \le m_j$ as well.

Let $\lambda := (\lambda_j, j \in \mathbb{N}_w)$ and $\mu := (\mu_j \geq 0, j \in \mathbb{N}_w)$ be the Lagrange multiplier vectors for the constraints $w_j = r(M_j - m_j + u_j)$ and $u_j \leq m_j, j \in \mathbb{N}_w$, respectively. Intuitively, w and λ decouple the computation of the utility company and that of individual EVs through coordination with the station operator. Additionally, μ decouples and coordinates all EVs' decisions so that EVs do not need direct communication among themselves to ensure that their decisions u_{aj} collectively satisfy $u_j \leq m_j$.

Consider the Lagrangian of Eq. (18) with these two sets of constraints relaxed:

$$L(x, u, \lambda, \mu) := f(x) + g(u) + \sum_{j \in \mathbb{N}_w} \lambda_j (w_j - r(M_j - m_j + u_j)) + \sum_{j \in \mathbb{N}_w} \mu_j (u_j - m_j) \quad (21)$$

and the dual problem of Eq. (18):

$$\max_{\lambda, \mu \geq 0} D(\lambda, \mu) := \min_{x \in \mathbb{X}, u \in \hat{\mathbb{U}}} L(x, u, \lambda, \mu)$$

where the constraint set $\hat{\mathbb{U}}$ on u is

$$\hat{\mathbb{U}} := \left\{ u \in \mathbb{R}^{AN_w} : u \text{ satisfies Eqs. (15a), (15b)} \right\}$$

Let $u_a := (u_{aj}, j \in \mathbb{N}_w)$ denote the vector of EV as decision on which station to swap its battery. Then the dual problem is separable in power flow variables x as well as individual EVs' decisions u_a:

$$D(\lambda, \mu) = V(\lambda) + \sum_{a \in \mathbb{A}} U_a(\lambda, \mu) \quad (22a)$$

where the problem $V(\lambda)$ solved by the utility company is

$$V(\lambda) := \min_{x \in \mathbb{X}} \left(f(x) + \sum_{j \in \mathbb{N}_w} \lambda_j w_j \right) \quad (22b)$$

and the problem $U_a(\lambda)$ solved by each individual EV a is

$$U_a(\lambda, \mu) := \min_{u_a \in \hat{\mathbb{U}}_a} \sum_{j \in \mathbb{N}_w} \left(\alpha d_{aj} - r\lambda_j + \mu_j \right) u_{aj} \quad (22c)$$

where the constraint set $\hat{\mathbb{U}}_a$ on u_a is

$$\hat{\mathbb{U}}_a := \left\{ u_a \in \mathbb{R}^{N_w} : \begin{array}{c} u_{aj} \in [0, 1], \ j \in \mathbb{N}_w \\ u_{aj} = 0 \quad \text{if } d_{aj} > \gamma_a c_a, \ j \in \mathbb{N}_w \\ \sum_{j \in \mathbb{N}_w} u_{aj} = 1 \end{array} \right\}$$

Note that Eq. (22c) has closed-form solutions. For instance, if there exists a unique optimal solution to $U_a(\lambda, \mu)$, that is, for any EV a there is a unique $j_a^*(\lambda, \mu)$ defined as

$$j_a^*(\lambda, \mu) := \arg \min_{j:\, d_{aj} \leq \gamma_a c_a} \{ \alpha d_{aj} - r\lambda_j + \mu_j \}$$

then the optimal solution can be uniquely determined as

$$u^*_{aj}(\lambda,\mu) := \begin{cases} 1, & \text{if} \quad j = j^*_a(\lambda,\mu) \\ 0, & \text{if} \quad j \neq j^*_a(\lambda,\mu) \end{cases}$$

that is, it simply chooses the unique station j^*_a within EV as driving range that has the minimum cost $\alpha d_{aj} - r\lambda_j + \mu_j$.

From Eq. (21), the standard dual algorithm for solving Eq. (18) is, for $j \in \mathbb{N}_w$,

$$\lambda_j(n+1) := \lambda_j(n) + \rho_1(n)[w_j(n) - r(M_j - m_j + u_j(n))] \tag{23a}$$

$$\mu_j(n+1) := \max\{\mu_j(n) + \rho_2(n)(u_j(n) - m_j), 0\} \tag{23b}$$

where $\rho_1(n), \rho_2(n) > 0$ are diminishing step sizes and, from Eq. (22), we have

$$x(n) := \arg\min_{x\in\mathbb{X}} \left(f(x) + \sum_{j\in\mathbb{N}_w} \lambda_j(n) w_j \right) \tag{23c}$$

and, for $a \in \mathbb{A}$,

$$u_a(n) := \arg\min_{u_a\in\hat{\mathbb{U}}_a} \sum_{j\in\mathbb{N}_w} \left(\alpha d_{aj} - r\lambda_j(n) + \mu_j(n)\right) u_{aj} \tag{23d}$$

Remark 2.

1. The x-update (23c) is carried out by the utility company and involves minimizing a convex objective with convex quadratic constraints. The only information that is nonlocal to the utility company for its x-update is one of the dual variables $\lambda(n)$ computed by the station operator.
2. The u_a-update (23d) is carried out by each individual EV. Each EV requires both the dual variables $(\lambda(n), \mu(n))$ from the station operator for its update.
3. The dual updates (23a), (23b) are carried out by the station operator which uses a (sub)gradient ascent algorithm to solve the dual problem $\max_{\lambda,\mu\geq 0} D(\lambda,\mu)$. It requires $w(n)$ from the utility company and individual decisions $u_a(n)$ from EVs a.

The communication structure is illustrated in Fig. 3. In particular, EVs are completely decoupled from the utility company and among themselves. Unlike the ADMM-based solution, the station operator knows only the battery swapping decisions of EVs, but not their private information such as locations (d_{aj}), states of charge (c_a), or performance (γ_a).

Since the relaxation (16) is convex, strong duality holds if Slater's condition is satisfied. Then, when the above (sub)gradient algorithm converges to a dual optimal solution (λ^*, μ^*), any primal optimal point is also a solution to the corresponding x-update (23c) and u_a-update (23d) [50, 51]. Suppose $(x(n), u_a(n), a \in \mathbb{A})$ indeed converges to a primal optimal solution $(x^*, u^*_a, a \in \mathbb{A})$, then typically $(u^*_a, a \in \mathbb{A})$ is not binary. However, the bound in Theorem 1 still holds that guarantees easy discretization and suggests that the final discretized stations assignments are close to optimum.

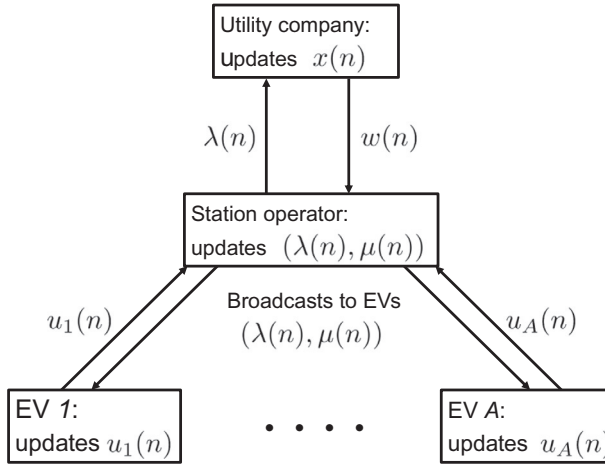

Fig. 3 Communication between utility company, station operator, and EVs.

Remark 3. The two solutions have their own advantages and can be adapted to different application scenarios. The ADMM-based solution requires a station operator that is trustworthy and can access EVs' private information. Since the station operator optimizes station assignments on behalf of all EVs, no computation is required on each EV, and meanwhile communication is only required between the station operator and the utility company. In contrast, the solution based on dual decomposition does not require sharing EVs' private information with the station operator. It does, however, necessitate computation capabilities on all EVs. In addition, communication is needed both between the station operator and the utility company and between the station operator and each EV.

5 Numerical results

5.1 Setup

We now evaluate the proposed algorithms through simulations using a 56-bus test system from SCE with a radial structure. Therefore, we will adopt the *DistFlow* equations to model power flows on the network. Similar performance can be anticipated on the other two models and is therefore skipped here. A maximum voltage deviation of 0.05 p.u. is allowed and all line capacities are set to infinity. More details about the test system can be found in [52, Fig. 2 and Table I]. We add four distributed generators and four stations at different buses, with parameters given in Table 1A. Note that the units of the real power, reactive power, cost, distance, and weight are MW, Mvar, $, km, and $/km, respectively. The four stations are assumed to be uniformly located in a 4 km $\times$ 4 km square area supplied by the test system, as shown in Table 1B. Two cases with different

TABLE 1 Setup.

(A) Distributed generator					
Bus	$\overline{p}_j^g$	$\underline{p}_j^g$	$\overline{q}_j^g$	$\underline{q}_j^g$	Cost function
1	4	0	2	−2	$0.3p^{g2} + 30p^g$
4	2.5	0	1.5	−1.5	$0.1p^{g2} + 20p^g$
26	2.5	0	1.5	−1.5	$0.1p^{g2} + 20p^g$
34	2.5	0	1.5	−1.5	$0.1p^{g2} + 20p^g$

(B) Station			
Bus	Location	M_j	m_j
5	(1, 1)	m_j	(i) A; (ii) $A/2$
16	(3, 1)	m_j	(i) A; (ii) $A/10$
31	(1, 3)	m_j	(i) A; (ii) $A/4$
43	(3, 3)	m_j	(i) A; (ii) $A/4$

m_js will be tested for illustration purposes. Suppose in a certain control interval, there are A EVs that request battery swapping (A will vary in our case studies). Their current locations are generated in a uniformly random manner within the square area while their destinations are ignored. We use the Euclidean distance for d_{aj}. We assume all EVs have sufficient battery energy to reach any of the four stations, which means that Eq. (8c) is readily satisfied. The extension to the general case where each EV has a limited driving range and can only reach some of the stations is straightforward. The constant charging rate is $r = 0.01$ MW [53] at all stations. We set the weight α to be 0.02 \$/km first [54]. For each case, we conduct 10 simulation runs with random EV locations. All numerical tests are run on a laptop with Intel Core i7-3632QM CPU@2.20 GHz, 8 GB RAM, and 64-bit Windows 10 OS.

5.2 Centralized solution

We first fix $M_j = m_j = A$, $j \in \mathbb{N}_w$, which means that in each station, batteries are all fully charged and sufficient to serve all EVs. The centralized solution is applied to two test cases with different numbers of EVs, and scalability analysis follows.

5.2.1 Nearest-station policy

Without optimization, the default policy is that all EVs head for their nearest stations to swap batteries. This is shown in Figs. 4A and 5A for two specific

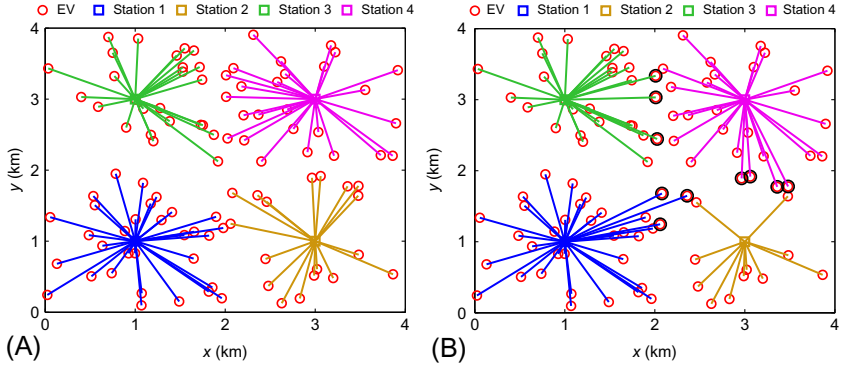

Fig. 4 #EVs = 100. (A) Nearest-station policy and (B) optimal assignments.

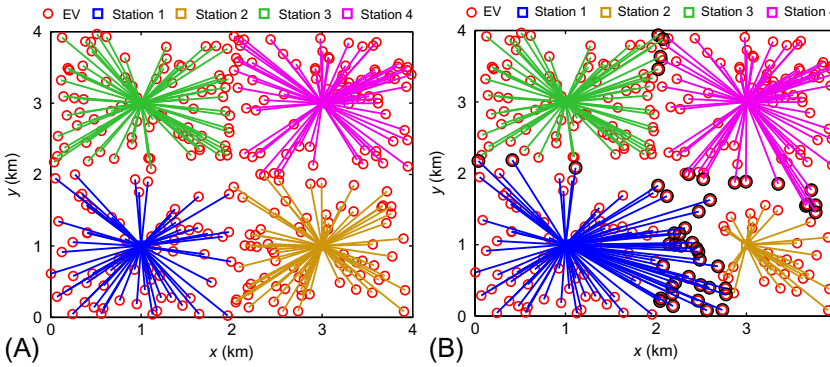

Fig. 5 #EVs = 300. (A) Nearest-station policy and (B) optimal assignments.

cases with 100 and 300 EVs, respectively. In practice this myopic policy can lead to a shortage in fully charged batteries at a station if many EVs cluster around that station due to correlations in traffic patterns. Moreover, it can cause voltage instability: the voltage magnitudes of some buses drop below the threshold 0.95 p.u. in the 300-EV case, as shown in Table 2, where the last column exhibits the resulting charging load at each bus.

5.2.2 *Optimal assignments*

Figs. 4B and 5B show the optimal assignments computed using the centralized solution for the previous two cases, respectively. The nearest stations are not assigned to some of the EVs (highlighted with thicker circles in the figures) when grid operational constraints such as voltage stability are taken into account. The number of such EVs is larger in the 300-EV case than that in the 100-EV case. The tradeoff between the EVs' travel distance and electricity generation cost is optimized. The OPF results of the 300-EV case are listed in Table 3 (compare

TABLE 2 Partial bus data under nearest-station policy (300 EVs).

Bus	$\lvert V_j \rvert$ (p.u.)	p_j^g	q_j^g	$r\sum_{a\in\mathbb{A}} u_{aj}$
1	1.050	0.571	0.000	/
4	1.047	2.500	0.663	/
5	1.031	/	/	0.660
16	0.941	/	/	0.700
18	0.948	/	/	/
19	0.944	/	/	/
26	1.050	2.500	0.410	/
31	1.020	/	/	0.830
34	1.044	2.500	1.500	/
43	1.015	/	/	0.810

TABLE 3 Partial bus data under optimal assignments (300 EVs).

Bus	$\lvert V_j \rvert$ (p.u.)	p_j^g	q_j^g	$r\sum_{a\in\mathbb{A}} u_{aj}$
1	1.050	0.520	0.000	/
4	1.048	2.500	0.590	/
5	1.025	/	/	0.990
15	0.981	/	/	/
16	0.974	/	/	0.300
17	0.980	/	/	/
18	0.973	/	/	/
19	0.969	/	/	/
26	1.050	2.500	0.439	/
31	1.019	/	/	0.840
34	1.044	2.500	1.500	/
43	1.013	/	/	0.870

with Table 2). As we can see from Table 3, the outputs (2.500 MW) of the distributed generators at buses 4, 26, and 34 have reached their full capacity (2.5 MW) while the injection (0.520 MW) at bus 1 (the substation bus) is far from its capacity (4 MW). This is consistent with our intuition that distributed

generations that are closer to users and potentially cheaper than power from the transmission grid are favored in OPF. Under the optimal assignments, the deviations of voltages from their nominal value are all less than 5%.

5.2.3 Optimality of generalized Benders decomposition

The upper and lower bounds on the optimal objective values for the previous two cases are plotted in Fig. 6 as the algorithm iterates between the master and slave problems. More iterations are required for larger-scale cases where the algorithm usually struggles longer to obtain an initial feasible solution. Once a feasible solution is found, the gap between the upper and lower bounds starts to shrink rapidly and the convergence to optimality is achieved within a few iterations.

5.2.4 Exactness of SOCP relaxation

We check whether the solution computed by generalized Benders decomposition attains equality in Eq. (6c), that is, whether the solution satisfies power flow equations and is implementable. Our result confirms the exactness of the SOCP relaxation for most cases we have tested on, including the previous two. Due to space limit, only partial data of the 300-EV case are shown in Table 4.

In summary, SOCP relaxation and generalized Benders decomposition seem to be effective in solving exactly our joint battery swapping and OPF problem (10).

5.2.5 Computational effort

To demonstrate the potential of the centralized solution for practical application, we check its required computational effort by counting its computation time for different numbers of EVs and stations, since the number of discrete variables in the optimization problem is the computational bottleneck. We use Gurobi to

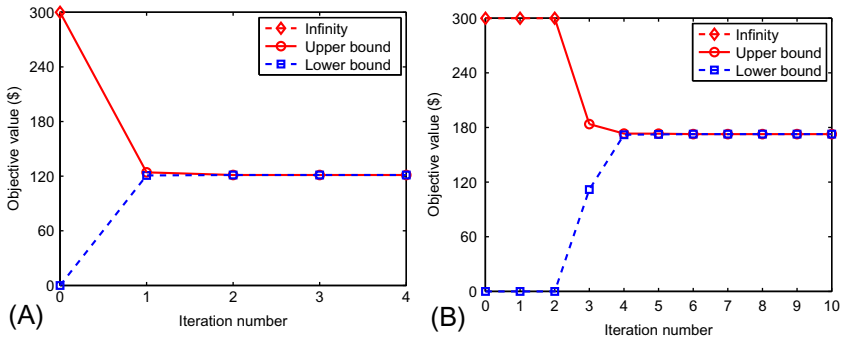

Fig. 6 Convergence of generalized Benders decomposition. (A) #EVs = 100. (B) #EVs = 300.

TABLE 4 Exactness of SOCP relaxation (partial results for 300 EVs).

Bus				
From	To	$v_j I_{jk}$	$\lvert S_{jk}\rvert^2$	Residual
1	2	0.271	0.271	0.000
2	3	0.006	0.006	0.000
2	4	0.202	0.202	0.000
4	5	1.369	1.369	0.000
4	6	0.005	0.005	0.000
4	7	1.952	1.952	0.000
7	8	1.691	1.691	0.000
8	9	0.009	0.009	0.000
8	10	1.269	1.269	0.000
10	11	1.092	1.092	0.000

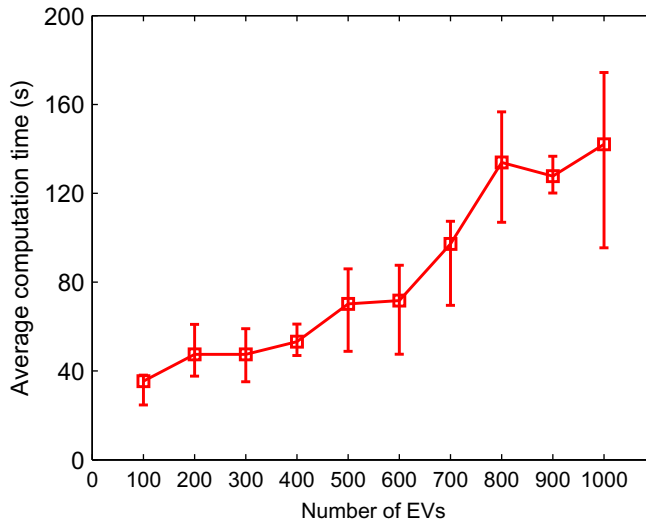

Fig. 7 Average computation time as a function of #EVs.

solve the master problem (integer programming) and SDPT3 to solve the slave problem (convex programming) on the MATLAB R2012b platform.

On the one hand, Fig. 7 shows the average computation time required by the centralized solution to find a global optimum for different numbers of EVs,

given the four fixed stations (note that each data point in Figs. 7–11 is an average over 10 simulation runs with random EV locations). On the other hand, we fix the number of EVs at 100 and scale up stations that are located at different randomly picked buses. Fig. 8 shows the average computation time required grows accordingly, but its sensitivity to the number of stations is moderate as the iterations that struggle for an initial feasible solution (recall Fig. 6) do not increase significantly when the number of EVs is fixed. Therefore, overall the required computational effort is desirable.

5.2.6 Benefit

Fig. 9 displays the average relative reduction in the objective value with different αs using optimal assignments, compared with the nearest-station policy. Scheduling flexibility is enhanced with more EVs, thus improving the savings. In addition, α expresses the system's relative emphasis on the two objective components. Clearly the smaller the weight α on EVs' travel distance is, the more benefit optimal assignments provide over the nearest-station policy. However, Fig. 9 also suggests that the improvement is small, that is, the nearest-station policy is good enough if it is implementable.

The nearest-station policy is sometimes infeasible either when there are more EVs nearest to a station than fully charged batteries at that station or when some operational constraints of the microgrid are violated. In our case studies, infeasibility is mainly due to some voltages dropping below the allowable lower limit. Define a metric *voltage drop violation* as VDV $:= \sum_{j\in\mathbb{N}} \max\{\sqrt{\underline{v}_j} - \sqrt{v_j}, 0\}$ to quantify the degree of voltage violation. Fig. 10 shows the average

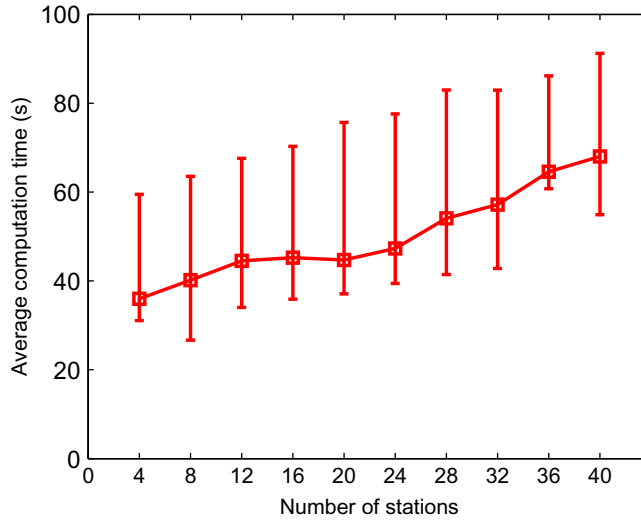

Fig. 8 Average computation time as a function of #stations.

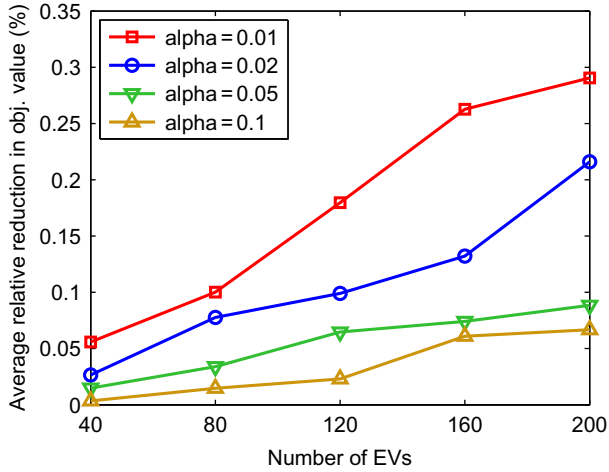

Fig. 9 Average relative reduction in objective value.

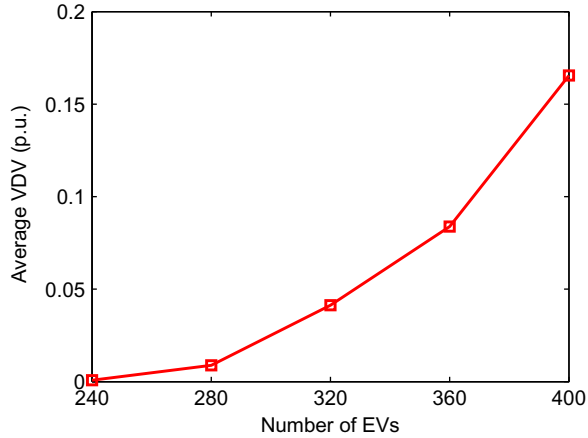

Fig. 10 Average VDV under nearest-station policy.

VDV for the number of EVs ranging from 240 to 400 under the nearest-station policy. The voltage violation becomes more severe when the number of EVs increases.

It is also interesting to look at cases where there are more EVs nearest to a station than fully charged batteries that station can provide, which, as far as we know, are common in practice. We reset $M_1 = m_1 = M_2 = m_2 = \frac{1}{2}A$ and $M_3 = m_3 = M_4 = m_4 = \frac{1}{8}A$ to simulate these situations. Hence the total number of fully charged batteries in the system is $\frac{5}{4}A$. Fig. 11A shows, for each station, the

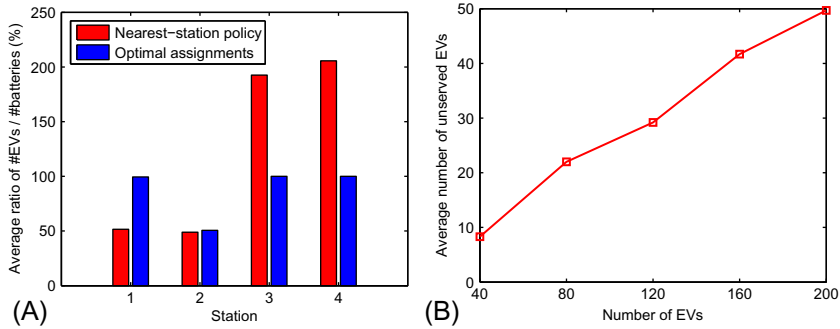

Fig. 11 (A) Average ratio of the number of forthcoming EVs to that of fully charged batteries. (B) Average number of unserved EVs under nearest-station policy.

average ratio of the number of EVs which go to the station for battery swapping to that of fully charged batteries at the station, under both the nearest-station policy and optimal assignments. In total, 99.40% of station 1's batteries, 50.60% of station 2's batteries, and all the batteries at stations 3 and 4 are used under the optimal assignments, thus they have collectively served all A EVs. Under the nearest-station policy, however, only 51.55% and 48.89% of stations 1 and 2's batteries, respectively (i.e., a total of around $\frac{1}{2}A$ batteries) are used for swapping. At either of stations 3 and 4, the number of EVs is approximately double that of available fully charged batteries (192.61% and 205.62%, respectively). Fig. 11B shows the average number of unserved EVs under the nearest-station policy as a function of the total number of EVs. On average, approximately one in four EVs cannot be served at their nearest stations, mainly due to congestion at stations 3 and 4, while available fully charged batteries at stations 1 and 2 are not fully utilized.

5.3 Distributed solutions

We first fix the number of EVs that request battery swapping as $A = 400$, and test the two cases with different m_js, listed in Table 1B, using our distributed solutions, followed by scalability analysis.

5.3.1 Convergence

The convergence of ADMM in case (i) is demonstrated in Fig. 12. Fig. 12A and B shows, respectively, that the Lagrange multiplier vector λ and the residual of the relaxed equality constraint (18c) converge rapidly. Case (ii) behaves similarly. Each iteration that computes the three steps of Eq. (20) takes on average 0.477 s by Gurobi. For the dual decomposition algorithm, Fig. 13A and B shows the convergence of its two Lagrange multiplier vectors λ and μ, respectively, in case (ii). λ maintains the consensus between the utility

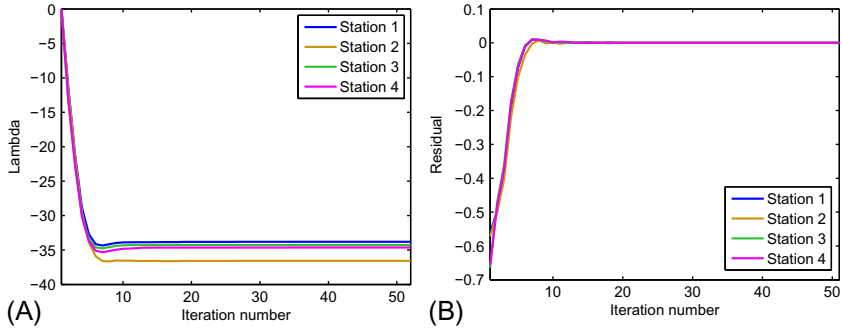

Fig. 12 Convergence of ADMM. (A) λ. (B) Residual of relaxed (18c).

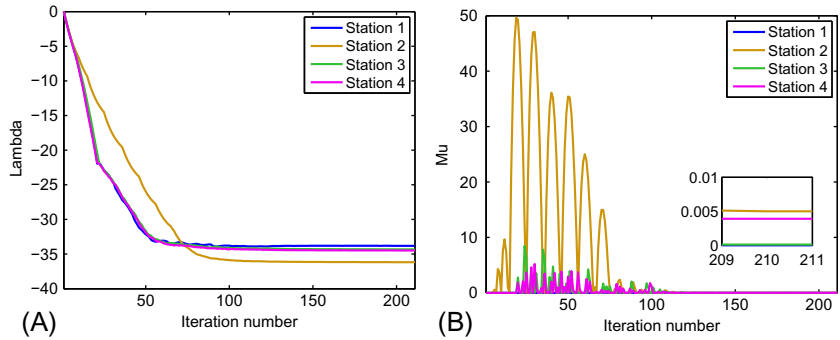

Fig. 13 Convergence of dual decomposition. (A) λ. (B) μ.

company and EVs at convergence, and μ guarantees (15c) is satisfied when it converges. Dual decomposition usually takes more iterations to converge due to the additionally required coordination among all EVs. For case (i), results are similar except that μ remains 0 during computation as Eq. (15c) is always satisfied. Each iteration of the dual decomposition algorithm involves the centralized update of Eqs. (23a), (23b) and the parallelized computation of Eqs. (23c), (23d). Each iteration takes on average 0.212 s by Gurobi.

5.3.2 Suboptimality (comparison with centralized solution)

In case (i), both algorithms obtain a solution in which the station assignments to two EVs, highlighted with thicker circles in Fig. 14A, are nonbinary: $u_{242} = [0.707\ 0.293\ 0.000\ 0.000]$ and $u_{367} = [0.230\ 0.000\ 0.770\ 0.000]$. This is consistent with Theorem 1. If we simply round u_{243} and u_{367} to binary values, the resulting solution turns out to coincide with a globally optimal solution computed using the centralized solution.

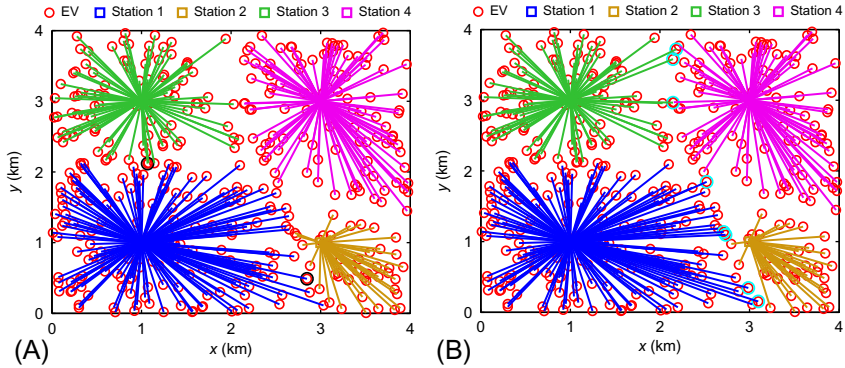

Fig. 14 Suboptimality in different cases. (A) Case (i). (B) Case (ii).

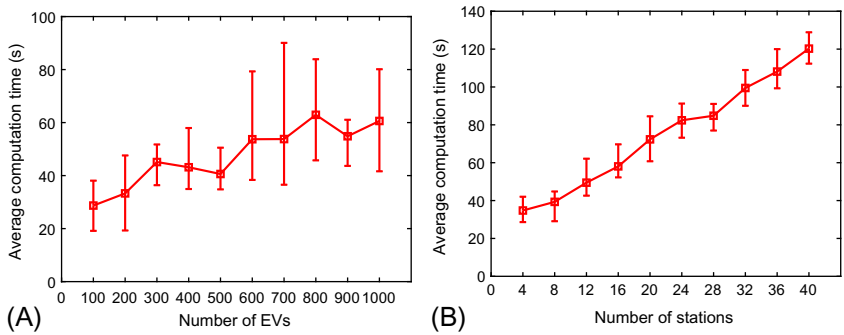

Fig. 15 Average computation time of ADMM. (A) As a function of #EVs. (B) As a function of #stations.

In case (ii), we reduce available fully charged batteries at each station to activate Eq. (15c). Fig. 14B shows the solution achieved by both algorithms. The solution turns out to be globally optimal for the original problem (10); in particular, all station assignments are binary. EVs, to which the station assignments are altered due to the bound imposed on battery availability of each station, are highlighted with thicker circles in Fig. 14B. The intuition is that an active (Eq. 15c) can sometimes help eliminate nonbinary assignments to EVs. This is often the case in practice where battery availability is uneven across stations.

5.3.3 *Exactness of SOCP relaxation*

In most cases that we have simulated, including cases reported here, the SOCP relaxation is exact, that is, the solutions computed by the two distributed algorithms attain equality in Eq. (6c) and therefore satisfy power flow equations. Partial data for case (ii) are listed in Table 5.

TABLE 5 Exactness of SOCP relaxation (partial results for case (ii)).

Bus				
From	To	$v_j I_{jk}$	$\lvert S_{jk}\rvert^2$	Residual
1	2	2.582	2.582	0.000
2	3	0.006	0.006	0.000
2	4	2.336	2.336	0.000
4	5	3.413	3.413	0.000
4	6	0.005	0.005	0.000
4	7	2.276	2.276	0.000
7	8	1.984	1.984	0.000
8	9	0.009	0.009	0.000
8	10	1.518	1.518	0.000
10	11	1.318	1.318	0.000

5.3.4 Scalability

We follow the same principle earlier for the centralized solution to demonstrate the scalability of the two distributed solutions, that is, we first augment the number of EVs while the number of stations is fixed and then turn it the other way round. The computation time that is shown in Figs. 15 and 16 is averaged over 10 simulation runs with randomly generated cases. Approximately, the computational effort of both solutions increases linearly as EVs (or stations) scale up. Compared with the centralized solution, the required computation time

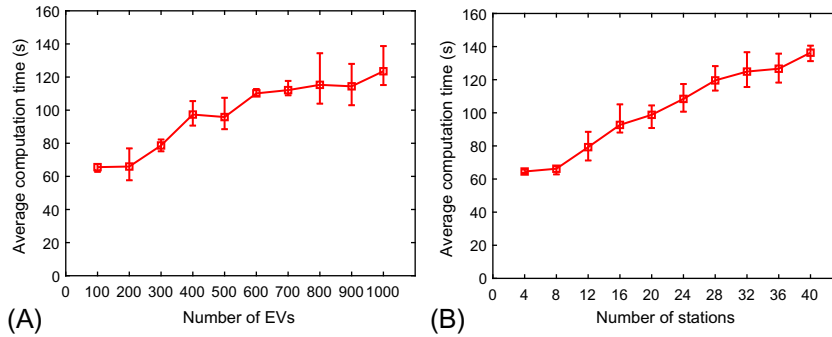

Fig. 16 Average computation time of dual decomposition. (A) As a function of #EVs. (B) As a function of #stations.

of the distributed solutions is less sensitive to the EV scale, which is intuitive, but turns out to be more sensitive to the station scale. This results from the fact that the consensus that the distributed solutions strive toward has to be achieved at each station. Generally, more iterations are needed as more stations are involved.

6 Concluding remarks

6.1 Summary

We formulate an optimal scheduling problem for battery swapping in a microgrid that assigns to each EV a best station to swap its depleted battery based on its current location and state of charge. The schedule aims to minimize a weighted sum of EVs' travel distance and electricity generation cost over both station assignments and power flow variables, subject to EV range constraints, grid operational constraints, and AC power flow equations. Three representative linearization or convex relaxation methods are discussed for modeling the power flows on the microgrid, based on which we then propose both centralized and distributed solutions to handle the binary nature of station assignments. The centralized solution is applicable to vertically integrated systems where global information and controllability are available. The distributed solutions are more suitable for systems where the distribution grid, stations, and EVs are operated by separate entities that do not share their private information. They allow these entities to make individual decisions but coordinate through privacy-preserving information exchanges. Numerical case studies on the SCE 56-bus test system validate our analysis and reveal some interesting results in potential practical application.

6.2 Model limitations

First, Assumption 1 is imposed by choosing a proper candidate set $\mathbb{A}$ of EVs when there is overwhelming demand of battery swapping, which significantly eases the model complexity at the sacrifice of a little performance. It will be interesting to model further the waiting cost of EVs when they cannot be immediately served at stations. Second, optimizing charging rates across intervals can be integrated to form a multiinterval scheduling problem if a good estimate of future information is available. Then it is worth evaluating the value of future information in improving the overall performance.

Appendix: Proof of Theorem 1

We refer to EV a as a *critical* EV if its station assignment satisfies $u_{aj} < 1$ for all $j \in \mathbb{N}_w$. We first show the following lemma and then prove Theorem 1. Let $(u, y) := (u, s^g, \phi)$.

Lemma 1. *It is always possible to find an optimal solution* (u^*, y^*) *to the relaxation (16) where no critical EVs share two stations, that is, there do not exist* $a, b \in \mathbb{A}$ *and* $j, k \in \mathbb{N}_w$ *such that* $u^*_{aj}, u^*_{ak}, u^*_{bj}, u^*_{bk} > 0$.

Proof. Fix any (u, y) that is feasible for Eq. (16). If $u_{aj}, u_{ak}, u_{bj}, u_{bk} > 0$ for some $a, b \in \mathbb{A}$ and $j, k \in \mathbb{N}_w$, we will construct station assignments u' that satisfy the lemma such that (u', y) is also feasible for Eq. (16) but has a lower or equal objective value. This proves the lemma.

Let $B_a := u_{aj} + u_{ak}$, $B_b := u_{bj} + u_{bk}$, $B_j := u_{aj} + u_{bj}$, and $B_k := u_{ak} + u_{bk}$. The interpretation of these quantities is that rB_a and rB_b are the charging loads of EVs a and b, respectively, and rB_j and rB_k are their load distributions at stations j and k, respectively. Clearly, $B_a + B_b = B_j + B_k$. Without loss of generality, we can assume either case 1: $B_a \geq B_j \geq B_k \geq B_b$ or case 2: $B_j \geq B_a \geq B_b \geq B_k$ holds. We now construct u' assuming case 1 holds. The construction is similar if case 2 holds instead.

We consider four disjoint subcases and construct u' for each subcase:

1.1 EV a is closer to station j but farther away from station k than b ($d_{aj} \leq d_{bj}, d_{bk} \leq d_{ak}$): Let $u'_{aj} = B_j, u'_{ak} = B_k - B_b, u'_{bj} = 0, u'_{bk} = B_b$ and the other variables remain the same as in (u, y). This means that the assignments u' send EV b to station k but not station j, and also increase the likelihood of EV a going to station j while decreasing that to station k. Since

$$\begin{aligned} u'_{aj} + u'_{ak} &= B_j + B_k - B_b = u_{aj} + u_{ak} \\ u'_{bj} + u'_{bk} &= B_b = u_{bj} + u_{bk} \\ u'_{aj} + u'_{bj} &= B_j = u_{aj} + u_{bj} \\ u'_{ak} + u'_{bk} &= B_k - B_b + B_b = u_{ak} + u_{bk} \end{aligned}$$

(u', y) is feasible Eq. (16). Moreover,

$$\begin{aligned} \sum_{c=a,b} \sum_{i=j,k} d_{ci} u'_{ci} &= d_{aj} B_j + d_{ak}(B_k - B_b) + d_{bk} B_b \\ &= d_{aj}(u_{aj} + u_{bj}) + d_{ak}(u_{ak} - u_{bj}) + d_{bk}(u_{bj} + u_{bk}) \\ &\leq \sum_{c=a,b} \sum_{i=j,k} d_{ci} u_{ci} - u_{bj}(d_{ak} - d_{bk}) \\ &\leq \sum_{c=a,b} \sum_{i=j,k} d_{ci} u_{ci} \end{aligned}$$

where the first inequality uses $d_{aj} \leq d_{bj}$ and the second inequality uses $d_{bk} \leq d_{ak}$. Therefore, (u', y) has a lower or equal objective value than (u, y).

1.2 EV b is closer to station j but farther away from station k than a ($d_{bj} \leq d_{aj}, d_{ak} \leq d_{bk}$): This case is symmetric to subcase 1.1.

1.3 EV a is closer than b to both stations ($d_{aj} \leq d_{bj}, d_{ak} \leq d_{bk}$): We have either $d_{bj} - d_{bk} \leq d_{aj} - d_{ak}$ or $d_{bj} - d_{bk} > d_{aj} - d_{ak}$. In the former case, let

$u'_{aj} = B_j - B_b, u'_{ak} = B_k, u'_{bj} = B_b, u'_{bk} = 0$. Then

$$\sum_{c=a,b}\sum_{i=j,k} d_{ci}u'_{ci} = \sum_{c=a,b}\sum_{i=j,k} d_{ci}u_{ci} + (d_{ak} - d_{bk} + d_{bj} - d_{aj})u_{bk}$$
$$\leq \sum_{c=a,b}\sum_{i=j,k} d_{ci}u_{ci}$$

Similar to subcase 1.1, (u', y) is feasible and has a lower or equal objective value. In the latter case, let $u'_{aj} = B_j, u'_{ak} = B_k - B_b, u'_{bj} = 0, u'_{bk} = B_b$. Then (u', y) is feasible and has a lower objective value.

1.4 EV b is closer than a to both stations ($d_{bj} \leq d_{aj}, d_{bk} \leq d_{ak}$): This case is symmetric to subcase 1.3.

This completes the proof of the lemma. □

Proof. Fix an optimal solution (u^*, y^*) to the relaxation (16) that satisfies Lemma 1. By definition, a critical EV splits its charging load between at least two different stations. An upper bound on the number of critical EVs is therefore the maximum number of critical EVs that we can assign the N_w stations to without violating Lemma 1.

Consider the set C_1 of critical EVs under the assignments u^* that split their charging loads between station $i = 1$ and (at least) another station $j = 2, \ldots, N_w$. Lemma 1 implies that there are at most $N_w - 1$ critical EVs in C_1 since the assignments u^* are optimal. Consider next the set C_2 of critical EVs not in C_1 that split their charging loads between station $i = 2$ and (at least) another station $j = 3, \ldots, N_w$. There are at most $N_w - 2$ critical EVs in C_2. Similarly there are at most $N_w - i$ critical EVs in the set C_i that are not in $\cup_{k=1}^{i-1} C_k$ that split their charging loads between station i and (at least) another station $j > i$. Hence the maximum number of such critical EVs is $(N_w - 1) + (N_w - 2) + \cdots + 1 = \frac{1}{2}N_w(N_w - 1)$. This completes the proof of Theorem 1. □

References

[1] P. You, S.H. Low, W. Tushar, G. Geng, C. Yuen, Z. Yang, Y. Sun, Scheduling of EV battery swapping—part I: centralized solution, IEEE Trans. Control Netw. Syst. 5 (4) (2018) 1887–1897.

[2] P. You, S.H. Low, L. Zhang, R. Deng, G.B. Giannakis, Y. Sun, Z. Yang, Scheduling of EV battery swapping—part II: distributed solutions, IEEE Trans. Control Netw. Syst. 5 (4) (2018) 1920–1930.

[3] C2ES, Climate TechBook, Center for Climate and Energy Solutions, US, 2016, Available from: www.c2es.org/energy/use/transportation, Accessed in Apr 2017.

[4] R.-C. Leou, C.-L. Su, C.-N. Lu, Stochastic analyses of electric vehicle charging impacts on distribution network, IEEE Trans. Power Syst. 29 (3) (2014) 1055–1063.

[5] T. Shang, Y. Chen, Y. Shi, Orchestrating ecosystem co-opetition: case studies on the business models of the EV demonstration programme in China, in: D. Beeton, G. Meyer (Eds.), Electric Vehicle Business Models. Lecture Notes in Mobility, Springer, Cham, 2015.

[6] Z. Ma, D.S. Callaway, I.A. Hiskens, Decentralized charging control of large populations of plug-in electric vehicles, IEEE Trans. Control Syst. Technol. 21 (1) (2013) 67–78.
[7] L. Gan, U. Topcu, S.H. Low, Optimal decentralized protocol for electric vehicle charging, IEEE Trans. Power Syst. 28 (2) (2013) 940–951.
[8] A. O'Connell, D. Flynn, A. Keane, Rolling multi-period optimization to control electric vehicle charging in distribution networks, IEEE Trans. Power Syst. 29 (1) (2014) 340–348.
[9] Y. Zhou, D.K.Y. Yau, P. You, P. Cheng, Optimal-cost scheduling of electrical vehicle charging under uncertainty, IEEE Trans. Smart Grid 9 (5) (2018) 4547–4554.
[10] S. Chen, L. Tong, iEMS for large scale charging of electric vehicles: architecture and optimal online scheduling, in: Proceedings of IEEE International Conference on Smart Grid Communications (SmartGridComm), 2012, pp. 629–634.
[11] J. Rivera, P. Wolfrum, S. Hirche, C. Goebel, H.-A. Jacobsen, Alternating direction method of multipliers for decentralized electric vehicle charging control, in: Proceedings of IEEE Conference on Decision and Control (CDC), 2013, pp. 6960–6965.
[12] J. Rivera, C. Goebel, H.A. Jacobsen, Distributed convex optimization for electric vehicle aggregators, IEEE Trans. Smart Grid 8 (4) (2017) 1852–1863.
[13] Z. Yang, T. Guo, P. You, Y. Hou, S.J. Qin, Distributed approach for temporal-spatial charging coordination of plug-in electric taxi fleet, IEEE Trans. Ind. Inf. 15 (6) (2019) 3185–3195.
[14] R. Li, Q. Wu, S.S. Oren, Distribution locational marginal pricing for optimal electric vehicle charging management, IEEE Trans. Power Syst. 29 (1) (2014) 203–211.
[15] Y. Zhang, P. You, L. Cai, Optimal charging scheduling by pricing for EV charging station with dual charging modes, IEEE Trans. Intell. Transp. Syst. 20 (9) (2019) 3386–3396.
[16] Z. Yu, S. Li, L. Tong, On market dynamics of electric vehicle diffusion, in: Proceedings of the 52nd Annual Allerton Conference on Communication, Control, and Computing, 2014, pp. 1051–1057.
[17] S. Sojoudi, S.H. Low, Optimal charging of plug-in hybrid electric vehicles in smart grids, in: Proceedings of IEEE Power & Energy Society General Meeting, 2011, pp. 1–6.
[18] L. Zhang, V. Kekatos, G.B. Giannakis, Scalable electric vehicle charging protocols, IEEE Trans. Power Syst. 32 (2) (2017) 1451–1462.
[19] N. Chen, C.W. Tan, T.Q.S. Quek, Electric vehicle charging in smart grid: optimality and valley-filling algorithms, IEEE J. Sel. Top. Sign. Process. 8 (6) (2014) 1073–1083.
[20] J. de Hoog, T. Alpcan, M. Brazil, D.A. Thomas, I. Mareels, Optimal charging of electric vehicles taking distribution network constraints into account, IEEE Trans. Power Syst. 30 (1) (2015) 365–375.
[21] J.F. Franco, M.J. Rider, R. Romero, A mixed-integer linear programming model for the electric vehicle charging coordination problem in unbalanced electrical distribution systems, IEEE Trans. Smart Grid 6 (5) (2015) 2200–2210.
[22] X. Tan, B. Sun, D.H.K. Tsang, Queueing network models for electric vehicle charging station with battery swapping, in: Proceedings of IEEE International Conference on Smart Grid Communications (SmartGridComm), 2014, pp. 1–6.
[23] S. Yang, J. Yao, T. Kang, X. Zhu, Dynamic operation model of the battery swapping station for EV (electric vehicle) in electricity market, Energy 65 (2014) 544–549.
[24] P. You, Z. Yang, Y. Zhang, S.H. Low, Y. Sun, Optimal charging schedule for a battery switching station serving electric buses, IEEE Trans. Power Syst. 31 (5) (2016) 3473–3483.
[25] M.R. Sarker, H. Pandžić, M.A. Ortega-Vazquez, Optimal operation and services scheduling for an electric vehicle battery swapping station, IEEE Trans. Power Syst. 30 (2) (2015) 901–910.

[26] Y. Zheng, Z.Y. Dong, Y. Xu, K. Meng, J.H. Zhao, J. Qiu, Electric vehicle battery charging/swap stations in distribution systems: comparison study and optimal planning, IEEE Trans. Power Syst. 29 (1) (2014) 221–229.
[27] X. Zhang, R. Rao, A benefit analysis of electric vehicle battery swapping and leasing modes in China, Emerg. Mark. Finance Trade 52 (6) (2016) 1414–1426.
[28] P. You, S.H. Low, Z. Yang, Y. Zhang, L. Fu, Real-time recommendation algorithm of battery swapping stations for electric taxis, in: Proceedings of IEEE Power & Energy Society General Meeting, 2016, pp. 1–5.
[29] P. You, J.Z.F. Pang, M. Chen, S.H. Low, Y. Sun, Battery swapping assignment for electric vehicles: a bipartite matching approach, in: Proceedings of IEEE Conference on Decision and Control (CDC), 2017, pp. 1421–1426.
[30] P. You, P. Cheng, J.Z.F. Pang, S.H. Low, Efficient online station assignment for EV battery swapping, in: Proceedings of ACM International Conference on Future Energy Systems (e-Energy), 2018, pp. 383–385.
[31] P. McDaniel, S. McLaughlin, Security and privacy challenges in the smart grid, IEEE Secur. Priv. 7 (3) (2009) 75–77.
[32] G. Kalogridis, C. Efthymiou, S.Z. Denic, T.A. Lewis, R. Cepeda, Privacy for smart meters: towards undetectable appliance load signatures, in: Proceedings of IEEE International Conference on Smart Grid Communications (SmartGridComm), 2010, pp. 232–237.
[33] C. Efthymiou, G. Kalogridis, Smart grid privacy via anonymization of smart metering data, in: Proceedings of IEEE International Conference on Smart Grid Communications (SmartGridComm), 2010, pp. 238–243.
[34] E. Liu, P. You, P. Cheng, Optimal privacy-preserving load scheduling in smart grid, in: Proceedings of IEEE Power & Energy Society General Meeting, 2016, pp. 1–5.
[35] L. Yang, X. Chen, J. Zhang, H.V. Poor, Optimal privacy-preserving energy management for smart meters, in: Proceedings of IEEE Conference on Computer Communications (INFOCOM), 2014, pp. 513–521.
[36] H.-R. Tseng, A secure and privacy-preserving communication protocol for V2G networks, in: Proceedings of IEEE Wireless Communications and Networking Conference (WCNC), 2012, pp. 2706–2711.
[37] H. Liu, H. Ning, Y. Zhang, L.T. Yang, Aggregated-proofs based privacy-preserving authentication for V2G networks in the smart grid, IEEE Trans. Smart Grid 3 (4) (2012) 1722–1733.
[38] H. Nicanfar, P. TalebiFard, S. Hosseininezhad, V. Leung, M. Damm, Security and privacy of electric vehicles in the smart grid context: problem and solution, in: Proceedings of ACM International Symposium on Design and Analysis of Intelligent Vehicular Networks and Applications, 2013, pp. 45–54.
[39] M. Liu, R.H. Ordóñez-Hurtado, F. Wirth, Y. Gu, E. Crisostomi, R. Shorten, A distributed and privacy-aware speed advisory system for optimizing conventional and electric vehicle networks, IEEE Trans. Intell. Transp. Syst. 17 (5) (2016) 1308–1318.
[40] C. Clifton, M. Kantarcioglu, J. Vaidya, X. Lin, M.Y. Zhu, Tools for privacy preserving distributed data mining, ACM SIGKDD Explor. Newsl. 4 (2) (2002) 28–34.
[41] J. Zhou, X. Lin, X. Dong, Z. Cao, PSMPA: patient self-controllable and multi-level privacy-preserving cooperative authentication in distributed m-healthcare cloud computing system, IEEE Trans. Parallel Distrib. Syst. 26 (6) (2015) 1693–1703.
[42] A. Bernstein, E. Dall'Anese, Linear power-flow models in multiphase distribution networks, in: Proceedings of IEEE PES Innovative Smart Grid Technologies Conference Europe (ISGT-Europe), 2017, pp. 1–6.

[43] M.E. Baran, F.F. Wu, Optimal capacitor placement on radial distribution systems, IEEE Trans. Power Deliv. 4 (1) (1989) 725–734.
[44] S.H. Low, Convex relaxation of optimal power flow, I: formulations and relaxations, IEEE Trans. Control Netw. Syst. 1 (1) (2014) 15–27.
[45] S.H. Low, Convex relaxation of optimal power flow, II: exactness, IEEE Trans. Control Netw. Syst. 1 (2) (2014) 177–189.
[46] J.F. Benders, Partitioning procedures for solving mixed-variables programming problems, Numer. Math. 4 (1) (1962) 238–252.
[47] A.M. Geoffrion, Generalized benders decomposition, J. Optim. Theory Appl. 10 (4) (1972) 237–260.
[48] P. You, Z. Yang, M.Y. Chow, Y. Sun, Optimal cooperative charging strategy for a smart charging station of electric vehicles, IEEE Trans. Power Syst. 31 (4) (2016) 2946–2956.
[49] S. Boyd, N. Parikh, E. Chu, B. Peleato, J. Eckstein, Distributed optimization and statistical learning via the alternating direction method of multipliers, Found. Trends Mach. Learn. 3 (1) (2011) 1–122.
[50] S. Boyd, L. Xiao, A. Mutapcic, Subgradient methods, in: Lecture Notes of EE392O, vol. 2004, Stanford University, Autumn, Quarter, 2003, pp. 2004–2005.
[51] S. Boyd, L. Vandenberghe, Convex Optimization, Cambridge University Press, New York, 2004.
[52] M. Farivar, R. Neal, C. Clarke, S. Low, Optimal inverter VAR control in distribution systems with high PV penetration, in: Proceedings of IEEE Power & Energy Society General Meeting, 2012, pp. 1–7.
[53] M. Yilmaz, P.T. Krein, Review of battery charger topologies, charging power levels, and infrastructure for plug-in electric and hybrid vehicles, IEEE Trans. Power Electron. 28 (5) (2013) 2151–2169.
[54] EIA, Annual Energy Review, Energy Information Administration, US Department of Energy, 2011, Available from: www.eia.doe.gov/emeu/aer, Accessed in April 2017.